

# The carbon dioxide free power plant

Global climate change resulting from emissions of carbon dioxide and other green house gases is one of the greatest environmental problems of our time. Capture and storage of carbon dioxide has the potential to contribute to a significant and relatively quick reduction in CO2 emissions from power generation, allowing fossil fuels to be used as a bridge to a non-fossil future while taking advantage of the existing power-plant infrastructure. One capture technology is the oxy-fuel combustion process, which combines a conventional combustion process with a cryogenic air separation process. In the first part of this work, the oxy-fuel process is applied to commercial data from an 865 MWe lignite-fired reference power plant in Lippendorf, Germany. The second part focuses on the experimental and modeling work on the process carried out at the Chalmers 100 kW oxy-fuel test facility.

This report is a result from the project *Pathways to Sustainable European Energy Systems* – a five year project within The AGS Energy Pathways Flagship Program.

The project has the overall aim to evaluate and propose robust pathways towards a sustainable energy system with respect to environmental, technical, economic and social issues. Here the focus is on the stationary energy system (power and heat) in the European setting.

The AGS is a collaboration of four universities that brings together world-class expertise from the member institutions to develop research and education in collaboration with government and industry on the challenges of sustainable development.



THE CARBON DIOXIDE FREE POWER PLANT

THE AGS PATHWAY REPORTS 2006:EU2

# The carbon dioxide free power plant

Large scale capture and storage of carbon dioxide  
Process evaluation and test-facility measurements



The AGS brings leading technical universities together with industry and government to confront some of the world's greatest challenges.

The AGS is an international partnership of four leading universities: The Swiss Federal Institute of Technology, Massachusetts Institute of Technology, Chalmers University of Technology, and The University of Tokyo.



## FOUR UNIVERSITIES

The Alliance for Global Sustainability is an international partnership of four leading science and technology universities:

**CHALMERS** Chalmers University of Technology, was founded in 1829 following a donation, and became an independent foundation in 1994. Around 13,100 people work and study at the university. Chalmers offers Ph.D and Licentiate course programmes as well as MScEng, MArch, BScEng, BSc and nautical programmes.

Contact: Alexandra Priatna  
Phone: +46 31772 4959 Fax: +46 31772 4958  
E-mail: alexandra.priatna@ags.chalmers.se

**ETH** Swiss Federal Institute of Technology Zurich, is a science and technology university founded in 1855. Here 18,000 people from Switzerland and abroad are currently studying, working or conducting research at one of the university's 15 departments.

Contact: Peter Edwards  
Phone: +41 44 632 4330 Fax: +41 44 632 1215  
E-mail: peter.edwards@env.ethz.ch

**MIT** Massachusetts Institute of Technology, a coeducational, privately endowed research university, is dedicated to advancing knowledge and educating students in science, technology, and other areas of scholarship. Founded in 1861, the institute today has more than 900 faculty and 10,000 undergraduate and graduate students in five Schools with thirty-three degree-granting departments, programs, and divisions.

Contact: Karen Gibson  
Phone: +1 617 258 6368 Fax: +1 617 258 6590  
E-mail: kgibson@mit.edu

**UT** The University of Tokyo, established in 1877, is the oldest university in Japan. With its 10 faculties, 15 graduate schools, and 11 research institutes (including a Research Center for Advanced Science and Technology), UT is a world-renowned, research oriented university.

Contact: Yuko Shimazaki  
Phone: +81 3 5841 7937 Fax: +81 3 5841 2303  
E-mail: shimazaki@ir3s.u-tokyo.ac.jp

# The carbon dioxide free power plant

Large scale capture and storage of carbon dioxide  
Process evaluation and test-facility measurements

AGS Pathways report 2006:EU2

*This report is based on a thesis work made by Klas Andersson  
at the Department of Energy and Environment, Division  
of Energy Technology, at Chalmers University of Technology*

PATHWAYS TO SUSTAINABLE EUROPEAN ENERGY SYSTEMS  
AGS, THE ALLIANCE FOR GLOBAL SUSTAINABILITY

Göteborg 2006

This report can be ordered from:

AGS Office at Chalmers

GMV, Chalmers

SE - 412 96 Göteborg

[alexandra.priatna@chalmers.se](mailto:alexandra.priatna@chalmers.se)

# The carbon dioxide free power plant

Large scale capture and storage of carbon dioxide  
Process evaluation and test-facility measurements

Copyright 2006

Produced by Kreativ Media AB

Editing Lars Magnell

Layout Måns Ahnlund

Printed by PR-Offset, Mölndal

ISBN 978-91-976327-0-6

# Table of content

Introduction	1
--------------	---

## Part 1

■ Method	6
■ Results	8
■ Plant Efficiency and Emissions	13
■ Economic evaluation	15
■ Conclusions	18

## Part 2

■ Aim of Experimental work	20
■ Experimental facility and test conditions	24
■ Measurements	27
■ Results and discussion	30
■ On-going work on oxy-coal combustion	37
■ Conclusions	39

Appendix	40
----------	----

■ Pathways to sustainable European energy systems	45
■ The Alliance for Global Sustainability	47



# Introduction

Global climate change resulting from emissions of carbon dioxide and other greenhouse gases is one of the greatest environmental problems of our time.

In order to stabilize the atmospheric concentrations of greenhouse gases drastic cuts in particularly carbon dioxide emissions are required.

Carbon dioxide, CO<sub>2</sub>, is by far the most dominant greenhouse gas, and approximately 80 percent of the anthropogenic emission of CO<sub>2</sub> is due to fossil fuel combustion.

Capture and storage of carbon dioxide has the potential to contribute to a significant and relatively quick reduction in CO<sub>2</sub> emissions from power generation, allowing fossil fuels to be used as a bridge to a non-fossil

future while taking advantage of the existing power-plant infrastructure.

## **Oil recovery**

At present there are no power plants with carbon dioxide capture available on a commercial scale, but long time aquifer storage is currently applied and evaluated in the North Sea showing promising results. Carbon dioxide could also be stored in connection to

enhanced oil recovery or enhanced coal bed methane recovery to make up for some of the economic losses associated with the energy penalty of the capture processes.

## **The oxy-fuel combustion process**

New technologies can be used in capture plants for combustion of fossil fuel with subsequent capture and storage of carbon dioxide. One such







technology is the oxy-fuel combustion process, which combines a conventional combustion process with a cryogenic air separation process, so that the fuel is burnt in oxygen and recycled flue gas. This results in a high concentration of carbon dioxide in the flue gas, which reduces the cost for its capture. Other commonly studied processes are amine-based absorption processes and the integrated gasification combined cycle.

### **The Lippendorf plant**

In the first part of this work, the oxy-fuel process is applied to commercial data from an 865 MWe lignite-fired reference power plant in Lippendorf, Germany, and large air separation units (ASU).

A detailed design of the flue gas treatment pass, integrated in the overall process layout, is proposed. Essential components and energy streams of the two processes have been investigated in order to evaluate the possibilities for process integration and to determine the net efficiency of the capture plant.

The electricity generation cost and

the associated avoidance cost for the capture plant have been determined and compared to the reference plant with investment costs obtained directly from industry. Although an existing reference power plant forms the basis of the work, the study is directed towards a new state-of-the-art lignite-fired oxy-fuel power plant. The boiler power of the capture plant has been increased to keep the net output of the capture and the reference plant similar.

The second part of the report focuses on the experimental and modeling work on the combustion process carried out at Chalmers. The experiments are performed in the Chalmers 100 kW oxy-fuel test facility. The overall aim of this work is to increase the knowledge on the combustion fundamentals and to generate data and modeling tools required in the design of a commercial scale oxy-fuel fired power boiler.

### **Combined capture**

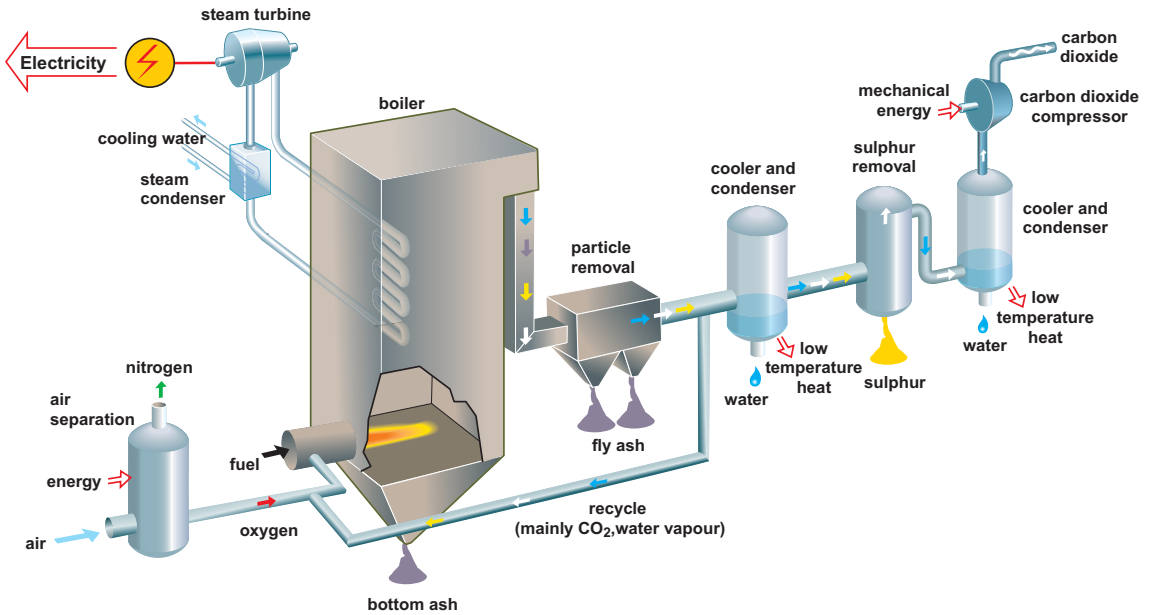
Both absorption based capture processes and oxy-fuel combustion are often considered as alternatives for

retro-fitting of existing coal-fired units making it possible to take advantage of already invested capital which to a certain extent can be considered as sunk costs. However, existing units are often old units with rather modest net efficiencies and with the increased parasitic losses of the capture, the retrofit concept results in comparatively high fuel costs. It should therefore be pointed out that although an existing reference power plant has been the basis of the process design of this study, the present work should be considered as a process evaluation for a new oxy-fuel fired power plant, with all its components and costs. Furthermore, as a comparison the associated costs are determined for a capture plant both with and without a sulphur dioxide removal system (wet flue gas desulphurization) in order to show the possible economic benefit from combined capture of sulphur dioxide and carbon dioxide – in the case this will be environmentally approved and applicable to the type of storage. considered.

### **Coal-mining in Germany**

The International Energy Agency (IEA) predicts that renewable energy sources, such as wind power, will continue to represent less than 15 per cent of world consumption for another 20 to 30 years. In the EU (EU-25) the use of fossil fuels is foreseen to increase. According to the IEA reference scenarios, 50–60 per cent of the electricity and heat will be based on fossil fuels in 2030, compared to 55 per cent in 2002.

## O<sub>2</sub>/CO<sub>2</sub> recycle (oxyfuel) combustion capture



The oxy-fuel combustion process is applicable to different types of fuels and boilers. It involves burning the fuel in an atmosphere of carbon dioxide and recycled flue gas instead of in air, as outlined in the figure above.

The mixed flow of oxygen and recycled flue gas is fed to the boiler together with the fuel, which is burnt as in a conventional plant. Typically 70-80 percent of the flue gas is recycled from down stream the economizer and mixed with new oxygen. The remaining part of the flue gas is cleaned, compressed and later transported to storage or to another application.

# Part 1

# Method

The 2 x 865 MW lignite-fired Lippendorf power plant in northern Germany is used as reference in this study. This is a modern state of the art power plant commissioned in the year 1999.

Process data and schemes were obtained directly from the plant owner. Based on these data, a process evaluation was carried out in order to identify new components needed as well as components that can be excluded from the reference boiler scheme.

The process layout is based on an existing air separation unit with an oxygen production of 50,000 cubic meters per hour.

## Different coal qualities

Two different chemical process simulation programs, ChemCad and

Hysys were used to simulate the chemical reactions in the flue gas condenser for cross comparison of results. ChemCad, which in this case is the most accurate one, uses electrolyte reactions together with thermodynamic models (Peng-Robinson). Hysys does not consider the electrolyte reactions and hence, for dissolved compounds the accuracy is lower than in the Chemcad program.

The actual fuel flow and coal composition at the Lippendorf plant is adapted to three different coal qualities: a guarantee coal and the so-called max water and max ash coals. The guaran-

tee coal is used for all calculations regarding efficiency and flue gas flows. The plant must nevertheless be able to handle other coal as well. Thus “max ash” and “max water” coals are used for dimensioning the flue gas cleaning equipment.

## Flue gas desulphuration

All investment costs have been determined in co-operation with industry. The specific investment cost and variable operation and maintenance cost of the power plant with capture has been assumed equal to that of the reference power plant. In the

## Hysys and Refprop softwares

Different compressor configurations for the air separation unit, as well as for the flue gas compression were analyzed. Calculations of the adiabatic compressor work for different compressor cycle designs were performed using the software RefCalc from which pressure enthalpy diagrams and their corresponding numeric values are obtained.

The properties of the various gas mixtures are obtained from the NITS standard reference database with the software Refprop (Reference Fluid, Thermodynamic and Transport Properties).

Hysys was also used to determine the total heat rejection and the temperature curve of the condensation unit. In the proposed scheme, nitric oxide is separated in a liquid/gas separator since it is assumed not to be soluble in the liquid carbon oxy-fuel mixture.



The electricity generation cost and the associated avoidance cost for the capture plant have been determined and compared to the reference plant, the 2 x 865 MW lignite-fired Lippendorf plant, with investment costs obtained directly from industry. Although an existing reference power plant forms the basis of the work, the study is directed towards a new state-of-the-art lignite-fired oxy-fuel power plant.

case where the flue gas desulphurization is included, the investment cost has been reduced to 60 percent of the corresponding flue gas desulphurization for the reference plant, since the flue gas flow will drastically decrease in the oxy-fuel scheme. According to the literature wet flue gas desulphurization technology can be applied although the sulphur dioxide removal is to be performed in a carbon dioxide atmosphere with three times as high volumetric concentrations of sulphur dioxide compared to normal conditions in air firing.

### 95 percent oxygen purity

The investment and running costs of the air separation unit has been updated for the increased plant size. These costs were obtained from three different unit sizes ranging from 276,900 to 528,700  $\text{mn}^3/\text{h}$  of oxygen. The specific power consumption of these air separation units ranges from

0.34 to 0.36  $\text{kW}/\text{mn}^3/\text{h}$  for a unit producing oxygen of 99,6 percent purity. The power consumption and the investment costs are reduced when a lower purity is required. In this study all the calculations are made for an oxygen purity of 95 percent. The reduction in power demand is about

1.6 percent whereas the reduction for the investment costs is 4 percent.

A cost analysis for each process part (power plant, air separation unit and FGCC – Flue Gas Cleaning and Compression) was set up in order to obtain the electricity generation cost and the avoidance cost.

**Table 1. Process data for the reference power plant Lippendorf (identical for both blocks).**

Gross electricity output	933 MW
Net electricity output	865 $\text{MW}_e$
Boiler power	2030 MW
District heat extraction	115 MW
Electricity net efficiency	42.6 %
Fuel	Raw lignite
Steam flow	672 $\text{kg}/\text{s}$
High pressure steam	554/258.5°C/bar
Intermediate steam pressure	583/49.7°C/ bar
Steam pressure at condenser discharge	0.038 bar

# Results

The main result from the process study is the detailed overall process layout shown in the figure below. Based on this layout, which includes possibilities for process integration, the net efficiency of the oxy-fuel power plant was determined.

Figure 2 gives a principal process scheme of the lignite fired oxy-fuel plant as obtained from the process evaluation, using the Lippendorf as reference plant.

The air separation unit is based on cryogenic air separation, which is the only separation technique, which can provide the oxygen flows required in large-scale coal combustion plants.

An oxygen production rate of 528,000  $\text{m}^3/\text{h}$  is required and can be split into either 2 or 4 air separation unit production lines with a corre-

sponding maximum production capacity per line of 277,000 or 138,000  $\text{m}^3/\text{h}$ . An oxygen purity of 95 percent is selected as the most favorable, since it gives an exchange rate (oxygen to oxygen) of 1.0 without nitrogen in the product gas, but with near 5 percent argon content. Thus, for oxygen purities lower than 95 percent, the oxygen contains nitrogen in addition to argon. The final power consumption of the air separation unit with the above features becomes 181 MWe. The compressor(s) in the air separation

unit, with intercooling in four steps, operates between ambient temperature and about 60°C. Without intercooling an air temperature of about 210°C is reached, with a heat rejection of about 1 MWt per MWe consumed, which could be used for feed water preheating or district heating. However, this would result in a significant decrease in compressor efficiency of approximately 20 percent, which makes this alternative unattractive.

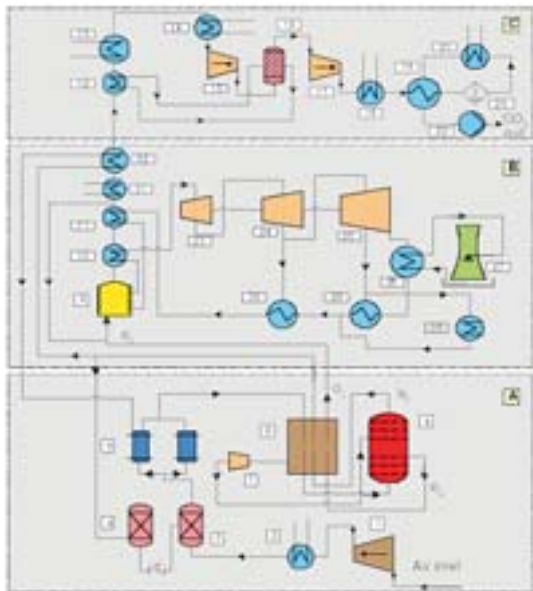


**Figure 2**

The three main parts of the plant are the air separation unit (A), the boiler island (B) and the flue gas treatment pass (C) with the essential features and components described below following the numbering of Figure 2.

- |                              |  |  |
|------------------------------|--|--|
| 1. Air compressor            | 12. TEG heat exchanger                                 | 23. HP Steam turbine                   |
| 2. Compressor cooling        | 13. Flue gas condensation unit                         | 24. IP Steam turbine                   |
| 3. Direct contact air cooler | 14. Flue gas cooler or FGD unit                        | 25. LP Steam turbine                   |
| 4. Evaporative cooler        | 15. Compressor unit 1, 30 bar                          | 26. Condenser                          |
| 5. Molecular sieves          | 16. TEG  | 27. Cooling tower                      |
| 6. Heat exchanger            | 17. Compressor unit 2, 58 bar                          | 28. District heating                   |
| 7. Expansion turbine         | 18. CO <sub>2</sub> condenser                          | 29. Feed water preheater (FPH)         |
| 8. Distillation column       | 19. Heat exchanger (CO <sub>2</sub> /CO <sub>2</sub> ) | 30. FPH                                |
| 9. Boiler                    | 20. Gas/Liquid separator                               | 31. Optional heater, district heat/FPH |
| 10. Super heater             | 21. Subcooler  | 32. Nitrogen heater                    |
| 11. Economizer               | 22. High pressure pump                                 |  |

## Cooling

The cooling of both the carbon dioxide compressors and the air compressor is carried out with cooling water from the plant cooling tower. In addition, the carbon dioxide condensation also requires cooling water from the cooling tower.

In total, there must be an almost 50 percent increase in mass flow of cooling water produced in the cooling towers compared to the reference plant in order to attain the low temperatures for the compressor inter cooling and the carbon dioxide condensation. However, if the temperature levels are increased only a few degrees the coolant mass flow will decrease significantly due to the narrow temperature intervals set in this study for the cooling of the components. To minimize losses in power transmission to the air and carbon dioxide compressors, these can be directly driven by steam turbines on a joint shaft.

**Table 2. Design composition of the flue gas during oxy-fuel combustion**

Components	[kg/s]	[wt%]	[mn <sup>3</sup> /s]	[vol%]
H <sub>2</sub> O	176.4	38.4	222.3	60.4
CO <sub>2</sub>	253.9	55.3	0.0	35.4
SO <sub>2</sub>	6.7	1.5	2.3	0.6
O <sub>2</sub>	6.4	1.4	142.1	1.2
N <sub>2</sub>	0.6	0.2	22.1	0.2
Ar	14.6	3.2	10.1	2.2
Total	458.7	100	416.9	100

However, the main steam turbine shaft cannot be used for this purpose, since it would cause problems both in the compressor units, such as surge at the start up, and in the shaft itself because of too large thermal motions.

The extra investment cost of the separate powering of the compressors

is to be compared with the power saving corresponding to about 0.7 percent of the net output.

The heat required in the molecular sieves are provided by the nitrogen heater, which exchanges heat from the flue gas with a minimum temperature of 200°C. A cooling capacity of about



Enormous amounts of carbon are naturally stored in the forest in trees and other plants, as well as in the forest soil. As part of photosynthesis trees absorb carbon dioxide from the atmosphere and store it as carbon while oxygen is released back into the atmosphere.

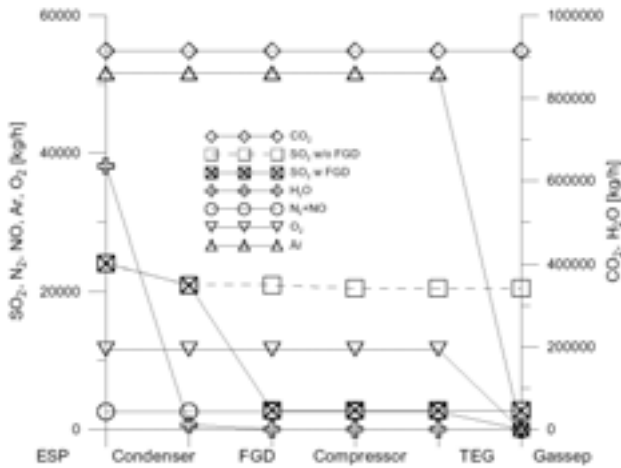


Figure 3 shows the mass flow of the flue gas components throughout the treatment steps with respect to excluding and including a flue gas desulphurization unit. Both options are provided since sulphur dioxide may cause problems depending on the type of storage considered. For example, storing of the sulphur dioxide below ground level can cause problems due to its sulphation behaviour in contact with calcium present in the storage environment. If sulphates are produced, in for example a saline aquifer, the porosity will decrease, which directly will affect the storage capacity.

25 MW at a temperature of 8°C, can be generated in the evaporative cooler that can be used in the flue gas treatment for sub cooling of the carbon dioxide

Table 2 (above) shows the flue gas mass and volume flows entering the flue gas treatment pass and the flue gas recycle loop in the oxy-fuel power plant. As seen wet recycling conditions are applied in the present process layout. This recycle approach will result in an increased level of sulphur dioxide and other impurities in the boiler. However, the advantage is that the flue gas flow entering the cleaning equipment is drastically reduced, which leads to savings in investment costs. Given that the flue gas desulphuriz-

ation is included in the process, no drastic changes on the overall design of the flue gas treatment would be required if, for fuel specific reasons mainly, dry and clean flue gas recycling conditions need to be applied. One such reason may be high concentrations of sulphur trioxide (SO<sub>3</sub>) causing the sulphuric acid dew point to drop. In principle the only difference is that the recycle line need to be changed to include flue gas condenser and a flue gas desulphurization unit and that the size of these two units must be increased to enable treatment of the total flue gas flow.

#### Preheating the feed water

Various options for the utilization of

the flue gas heat, available down stream of the economizer in the capture plant, have been evaluated. Heat available at a minimum temperature of 90°C could be used in an absorption cooler to produce a coolant stream at 5°C, for example to be used for sub-cooling purposes of the carbon dioxide or cooling of the compressors. Especially the large amount of heat rejected from the flue gas condenser, approximately 365 MW between 88°C and 60°C where the most part of the heat of evaporation is released, will require a heat sink. Part of this heat could be used in the available district heating system, but the one alternative represented in the results of this work is the integration with the steam cycle



to preheat the feed water instead of using low-pressure steam in order to increase the electricity output of the plant.

### Combined storage

The flue gas treatment basically involves the removal of water and non-condensable gases. A more or less complete dehydration of the flue gas is required to avoid problems in the final flue gas treatment pass and in the transportation of the captured carbon dioxide. Provided that the gas is dried to ppm level there is a technical possibility for combined storage of carbon dioxide and sulphur dioxide. This, since the physical behaviour of the two compounds is similar during supercritical conditions, for example

conditions required for the transport and the injection at the storage site. Such a capture plant could then exclude a sulphur dioxide removal system, which would result in some economic benefit.

### Complete dehydration

Besides technical feasibility, a combined underground storage of carbon dioxide and sulphur dioxide also depends on political decisions with respect to dumping conventions. A complete dehydration of the flue gas is important since it will reduce the mass flow, inhibit corrosion and hydrate precipitation. In the case of a combined storage of carbon dioxide and sulphur dioxide, provided that the flue gas is dehydrated to a dew point five

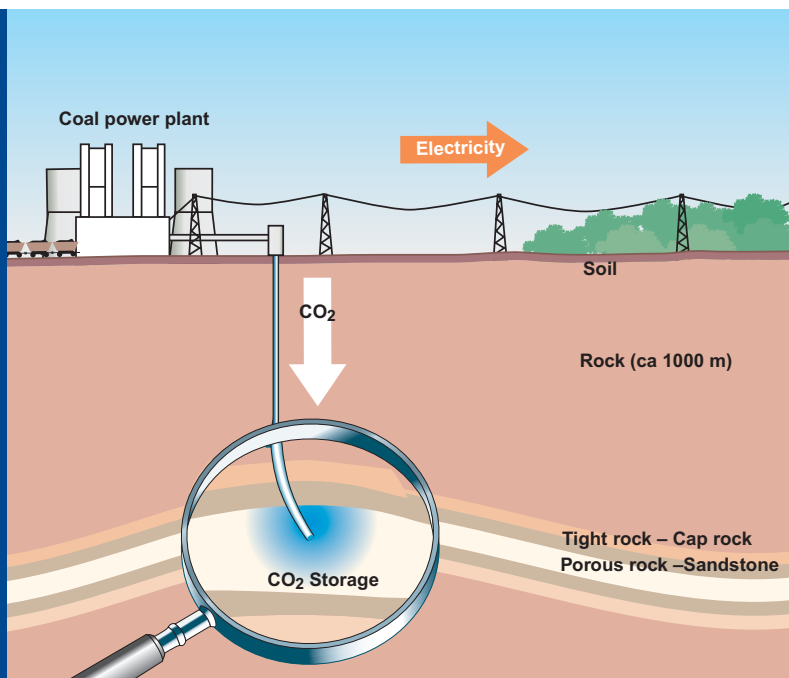
degrees below the temperature required for transport conditions, the sulphur dioxide will in principle behave as the carbon dioxide and the two gases will not cause any corrosion problems. For both storage options, the gas must nevertheless be dehydrated before reaching the high-pressure steps in the compression to make the compression of the gas mixture possible.

### Sweet corrosion

Carbon dioxide alone can be corrosive in the presence of water and cause so called sweet corrosion, that is when water vapour in the gas form solid ice-like crystals called gas hydrates. The hydrates are formed when water encages gas molecules smaller than 1.0



The idea is to capture CO<sub>2</sub> from a coal-fired power plant, transform it into a liquid, and permanently store it deep underground in suitable geological formations. The storages are of the same kind as where oil and gas have been stored for millions of years, a porous rock with an impermeable layer on top. At present several such storage tests are performed all over the world, for example beneath the sea or in the North Sea since 1996 (the SACS project) and also outside Berlin, where an abandoned gas storage exists (the CO<sub>2</sub>SINK project).



nm (which is the case for both carbon dioxide and sulphur dioxide) at low temperatures and elevated pressures (below 25°C and above 15 bar).

Various mechanisms for the carbon dioxide corrosion process have been proposed, which all involve either carbonic acid or bicarbonate ion formed when carbon dioxide is dissolved in water. Also in this case, dehydration to dew point five degrees below the transport temperature is sufficient to avoid the problem. This, since dry carbon dioxide is not corrosive at temperatures below 400°C. The maximum water content in the gas prior to compression should therefore not exceed 60 to 100 mg/m<sup>3</sup>, whatever the content of other possible acidic compounds. For pipeline transportation with presence of water, serious corrosion can be expected if

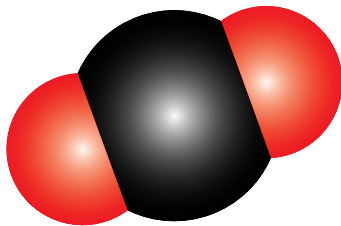
the partial pressure of carbon dioxide exceeds 2 bar.

#### Tri ethylene glycol unit

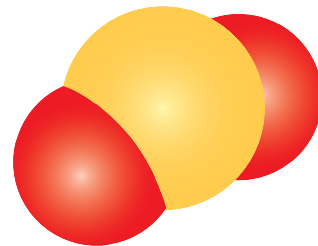
In the process chosen the gas is dehydrated in two steps. The first is in a traditional flue gas condenser where most of the water is removed, together with remaining particles (sulphur trioxide etc). The second dehydration step is the tri ethylene glycol unit, which will remove the remaining water down to a value of 60 mg/m<sup>3</sup>, corresponding to a dew point of -5°C at 100 bar under transport conditions. Since the tri ethylene glycol unit requires a pressure of 30 bar to be efficient, a compressor step with intercooling is installed before the unit. Some water is separated in the cooling steps in the compressor.

To reduce the power consumption

of the flue gas compressors, compression is carried out, up to the transport pressure, by a high-pressure pump. This, since the pressure should only be increased to a sufficient level, allowing transfer of the flue gas (mostly carbon dioxide) into a liquid state at a reasonable cost. The first compressor step raises the pressure from 1 bar to 30 bar, which is the inlet pressure of the tri ethylene glycol unit. The flue gas is then compressed in the second step from 30 bar to 58 bar. At a pressure of 58 bar, the carbon dioxide and sulphur dioxide will be liquefied, if cooled to 20°C by the main cooling system. When the carbon dioxide is liquefied a high-pressure pump is used for the last pressure increase up to 100 bar before transportation to the injection site.



Carbon dioxide



Sulphur dioxide

Besides technical feasibility, a combined underground storage of carbon dioxide and sulphur dioxide also depends on political decisions with respect to dumping conventions.


# Plant Efficiency and Emissions

The Sankey diagram below (figure 4) shows the reference power plant (a) and the oxy-fuel power plant (b). The figure illustrates the energy losses in the oxy-fuel plant with the same net electricity output as in the reference plant.

The net electrical efficiency of the plant becomes 33.5 percent, which is to be compared with 42.6 percent for the reference plant. The energy penalty of the capture plant consequently becomes 21.5 percent. The plant in the Sankey diagram represents the option

including sulphur dioxide removal. In the case of combined capture of sulphur dioxide and carbon dioxide the internal electricity demand is reduced, with a boiler power of 2524 MW and a net efficiency is slightly increased to 34.3 percent (see the power plant

specifications in Table 5 on page 17). The Sankey diagram of the capture plant includes the reduced power demand from a reduced flue gas flow as well as the integration possibilities as discussed previously. The electricity production is increased by about 10



Oceans are natural  
carbon dioxide sinks.

MW due to feed water preheating with heat from the flue gas condensation.

Table 3 summarizes emissions to the atmosphere from the oxy-fuel-fired plant obtained in the present study and

compares these with those of the reference plant. The combustion conditions are considered to be stoichiometric with an oxygen excess of 1.5 percent on a dry basis.

The sulphur oxide, nitric oxide and carbon dioxide emissions are leakage flows and ventilated flows from the flue gas treatment pass.

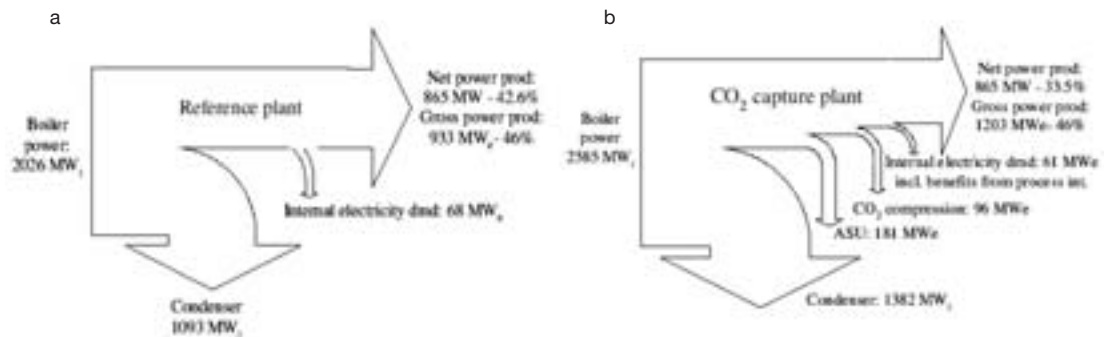


**Figure 4.** The Sankey diagrams of  
a) the reference power plant and  
b) The capture plant with the same power output as in the reference power plant.

**Table 3. Comparison of emissions to atmosphere between the reference plant and the oxy-fuel power plant.**

Emissions to air	Reference plant			oxy-fuel-plant		
	[mg/m <sup>3</sup> ]	[kg/h]	[kg/MWhe]	[mg/m <sup>3</sup> ]	[kg/h]	[kg/MWhe]
SO <sub>x</sub>	<350	<1120	1,28	<6	<13	0,015
NO <sub>x</sub>	<145	<460	0,53	<141	<190	0,220
CO <sub>2</sub>	<235	<740 000	855,2	<4	<5000	5,8
Dust	<2	<6	0,007	<1	<1	0,001

Estimation on nitric oxide with a reduction of the emission of about 60 percent. The reduction can be attributed to the absence of thermal nitric oxide as well as a drastic reduction in the conversion ratio of fuel-N to exhausted nitric oxide. The emitted nitric oxide is ventilated to air in a concentrated stream in the gas/liquid separator (as shown in figure 2, in section C) since it is assumed non-soluble in the carbon dioxide/sulphur dioxide mixture. In order to reach further reduction in nitric oxide emissions the high nitric oxide concentration stream should be well suited for a nitric oxide catalystr.

# Economic evaluation

The following pages give a brief outline of the economic parameters that determine the carbon dioxide capture and avoidance costs. An interest rate of 10 percent has been assumed as a midrange.

Table 4 lists the overall cost parameters used together with the capture and avoidance costs.

An interest rate of 10 percent has been assumed as a mid range value compared to previously performed studies on the economics of carbon dioxide capture where interest rates between 7 and 15 percent have been assumed. This is also in line with the standard power plant economic and assessment criteria, introduced by IEA,

which suggests an interest rate set at 10 percent and an assumed load factor of 85 percent. However, according to OECD the long-term interest rate (10 year basis) is forecasted to around 4 percent in the Euro area (March, 2005), why Table 4, below, gives the carbon dioxide avoidance cost for different interest rates and fuel prices and obviously these parameters have a significant impact on the results.

It should hence be noted that this

figure is likely to be lower in European projects and in a previous work by the authors an interest rate of 6 percent was applied. Lignite price, economic lifetime of the plant and distribution of costs during construction are based on information from industry. The energy availability of the plant is 7 500 hour per year at full capacity, which corresponds to a load factor of 85 percent.

The electricity generation cost with

**Table 4. Input cost parameters**

	Cost parameters	
O&M cost assumptions	Power plant - variable [ /MWh]	1.0
	Power plant - fixed [%]	1.5
	air separation UNIT - fixed [%]	4.0
	Flue gas treatment fixed [%]	4.0
Distribution of costs over construction period: 4 yrs	1st yr	0.15
	2nd yr	0.30
	3rd yr	0.35
	4th yr	0.20
Interest rate [%]		10.0
Lignite price [ /MWh]		4.00
Exchange rate [\$ / ]		1.30
Plant economic life time [yrs]		20

flue gas desulphurization increases from 42.1 to 64.3 USD per MWh, which corresponds to a carbon dioxide avoidance cost of 26 USD per ton carbon dioxide (or 20 euro per ton carbon dioxide).

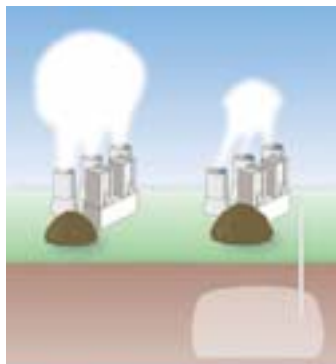
Without flue gas desulphurization the avoidance cost decreases about 4 USD per ton (3 euro per ton carbon dioxide).

**Marginal effect**

As previously discussed, storage of carbon dioxide contaminated with sulphur dioxide may be difficult from both a legal and public acceptance point of view. However, the results show that the combined storage has a marginal effect on the overall cost situation. It should be pointed out that the resulting cost is strongly dependent

on the economical parameters for the annuity cost calculations (although this should be rather obvious). The avoidance cost differ substantially both depending on the interest rate chosen for the invested capital and on the fuel cost. Thus, the latter should be kept in mind when comparing the results from the cost studies presented in the literature.





### CO<sub>2</sub> storage

The capacity to store carbon dioxide in Europe seems to exceed the needs based on available amounts of fossil fuels. The research on CO<sub>2</sub> storage is focused on three case scenarios:

1. On-shore geological storage near the power plant.
2. On-shore geological storage far away from the plant.
3. Off-shore geological storage beneath the sea floor in the North Sea.

**Table 5. Plant performance and costs of the reference plant and the oxy-fuel power plant with and without flue gas desulphurization (the cost of the flue gas desulphurization is included in the power plant cost).**

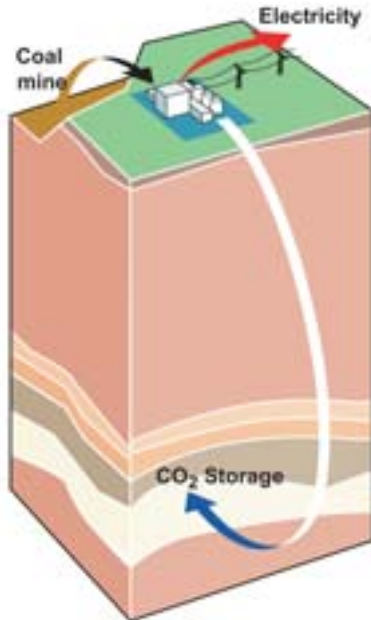
Plant performance and costs	Reference	oxy-fuel w. flue gas desulphurization	oxy-fuel w/o flue gas desulphurization
Boiler power [MW]	2026	2585	2524
Gross electrical output [MW]	933	1203	1176
Net electrical output [MW]	865	865	865
Operating time [h]	7500	7500	7500
Fuel demand [kg/s]	192.9	240.4	246.2
O <sub>2</sub> demand [kg/s]	-	221.6	226.9
<b>Total investment costs [10<sup>6</sup>x ]</b>			
Power plant	1100	1403.50	1310.74
Air separation UNIT	-	304.59	297.06
Flue gas treatment	-	35.46	34.70
Annualized capital cost [10 <sup>6</sup> x yr]	126.55	200.59	188.97
<b>O&amp;M costs: fixed + variable [10<sup>6</sup>x yr]</b>			
Power plant	22.99	29.33	27.39
Air separation UNIT	-	12.18	11.88
Flue gas treatment	-	1.42	1.39
Annualized O&M cost [10 <sup>6</sup> x yr/yr]	22.99	42.93	40.66
Fuel costs [10 <sup>6</sup> x yr/yr]	60.77	77.55	75.72
Total annualized costs [10 <sup>6</sup> x yr/yr]	210.31	321.07	305.35
Electricity generation cost [ /MWh]	32.4	49.5	47.1
Electricity generation cost [\$/MWh]	42.1	64.3	61.2
Emitted carbon dioxide [ton/MWh]	0.855	0.0058	0.0058
Avoidance cost [ /ton carbon dioxide]	-	20.0	17.1
Avoidance cost [\$/toncarbon dioxide]	-	26.0	22.3

# Conclusions

This study proposes an overall process scheme of an oxy-fuel plant based on commercial data for key components required in the process. With all integration possibilities considered the net efficiency becomes approximately 33.5 percent which should be compared to 42.6 percent in the reference plant. An almost complete dehydration of the flue gas is of great importance to avoid problems in the final flue gas treatment and in the transportation of the carbon dioxide. The fixed and running costs associated with an 865 MWe lignite-fired oxy-fuel power plant have been

evaluated in order to obtain the carbon dioxide avoidance cost for a new state-of-the-art capture plant. The capture plant has been scaled up to yield the same net capacity as the Lippendorf reference plant and the carbon dioxide emissions to the atmosphere are reduced with 99.5 percent. With a lignite price of 5.2 USD per MWh (4.0 euro per MWh) and an interest rate of 10 percent, the electricity generation cost increases from 42.1 to 64.3 USD per MWh which corresponds to a carbon dioxide avoidance cost of 26 USD per ton carbon dioxide (or 20 euro/ton

carbon dioxide). Furthermore, the study shows that if combined capture and storage of carbon dioxide and sulphur dioxide is environmentally approved and applicable to the type of storage considered, the economic benefit for the plant studied is still small with a reduction in the electricity generation cost of 3.1 USD per MWh. In summary, by using commercial data from existing plants and components this study shows that oxy-fuel combustion is a realistic and a near future option for carbon dioxide reductions in the power sector.



## Carbon dioxide Capture and Storage (CCS) technology in brief

The carbon dioxide ( $\text{CO}_2$ ) is captured from the power plant combustion process and compressed to liquid phase to make transportation easier. The  $\text{CO}_2$  is then transported to a storage site and injected into an underground porous rock formation for permanent storage at a depth of 800 metres or more. Here the carbon dioxide is maintained in a liquid state by the ambient pressure at that level.



# Part 2

# Aim of Experimental work

The second part of this report focuses on the experimental and modelling work on the combustion process carried out at Chalmers. The experiments are performed in the Chalmers 100 kW oxy-fuel test facility.

The overall objective of this work is to increase the knowledge on the combustion fundamentals and to generate data and modelling tools required in the design of a commercial scale oxy-fuel fired power boiler.

With this aim the Chalmers group works in close collaboration together with the University of Stuttgart, Vattenfall Utveckling AB and Fluent Europe in projects funded by the EU, the European power industry and the Swedish Energy Agency. One important near future activity, in which Chalmers participates, is the design and testing of the Vattenfall 30 MW oxy-fuel pilot plant, which is planned to be commissioned in the beginning of 2008.

## **Radiative heat transfer**

The work presented here summarizes the results from a recent study on flame characteristics of gas fired oxy-

fuel combustion where the focus is put on the radiative heat transfer of the flame and the combustion gases in the oxy-fuel environment. A description of the experimental equipment used for the measurements and the theory (see appendix) used for evaluating and analysing the radiative properties of the flame is given, followed by a description of the results from the study. Furthermore, a brief summary of the on-going work on oxy-coal combustion is given in the later part of this section. The experimental test unit facilitates oxy-fuel combustion with real flue gas recycling conditions. The gas-fired tests comprise a reference test in air and two oxy-fuel test cases with different recycled feed gas mixture concentrations of oxygen (21 and 27 volumepercent) and carbon dioxide (79 and 73 volumepercent). In-furnace gas concentration, temperature and total radiation (uni-directional) profiles are

presented and discussed. The change in total emissivity and gas emissivity of the oxy-fuel environment is discussed by means of available models and the experimental data.

## **Dry or wet mixtures**

In existing coal-fired power plants it is common that a small portion of the flue gases are externally recycled as a means to control the combustion temperature level in order to reduce the nitrogen oxide formation. For the oxy-fuel concept a high amount of recycled flue gas is required in order to maintain important combustion parameters, such as temperature, heat exchange, residence time and mixing conditions etc, on similar levels to those of air-fired combustion. The combustion will therefore take place in dry or wet mixtures of oxygen and carbon dioxide instead of in oxygen/nitrogen. The overall combustion



Front side of the Chalmers 100 kW oxy-fuel combustion test unit showing the top fired 3.0 meters high combustor. In the background to the left the fabric filter can be seen with the surrounding piping system.

behavior will, to a varying extent, be different from conventional combustion with possible changes in for example fuel burnout, ignition behavior, heat transfer and pollutant emissions. Apparently the differences are caused by the different physical and chemical properties of carbon dioxide compared to nitrogen. The experimental work performed elsewhere on oxy-fuel combustion mainly concerns the combustibility and emission formation of different type of coals for different mixtures of oxygen in either dry or wet recycled flue gas together with in-furnace measurements of species concentrations, temperatures and heat flux profiles. The work on such combustion characteristics has been carried out both in laboratory and semi-industrial scale test facilities.

### **Nitrogen oxide**

Previous work has concluded that coal-fired oxy-fuel combustion could be maintained under satisfactory conditions, that is conditions that would be applicable to existing utility boilers. More recent experimental work has focused on the gas phase reactions and overall emission characteristics for different coal types, and, especially so when it comes to formation and reduction of nitrogen oxide during either real or simulated flue gas recycling conditions. These studies indicate that the nitrogen oxide conversion ratio from fuel-N under oxy-fuel conditions can be reduced significantly compared

to air-fired conditions. One obvious reason to these results is that the no thermal nitrogen oxide is formed due to the absence of nitrogen in the feed gas. More detailed studies on the nitrogen chemistry for different types of coals and combustion atmospheres are however required to get a deeper understanding on the nitrogen oxide formation during oxy-fuel combustion.

Little data is available on the radiative properties of different mixtures of oxygen and carbon dioxide and fuels.

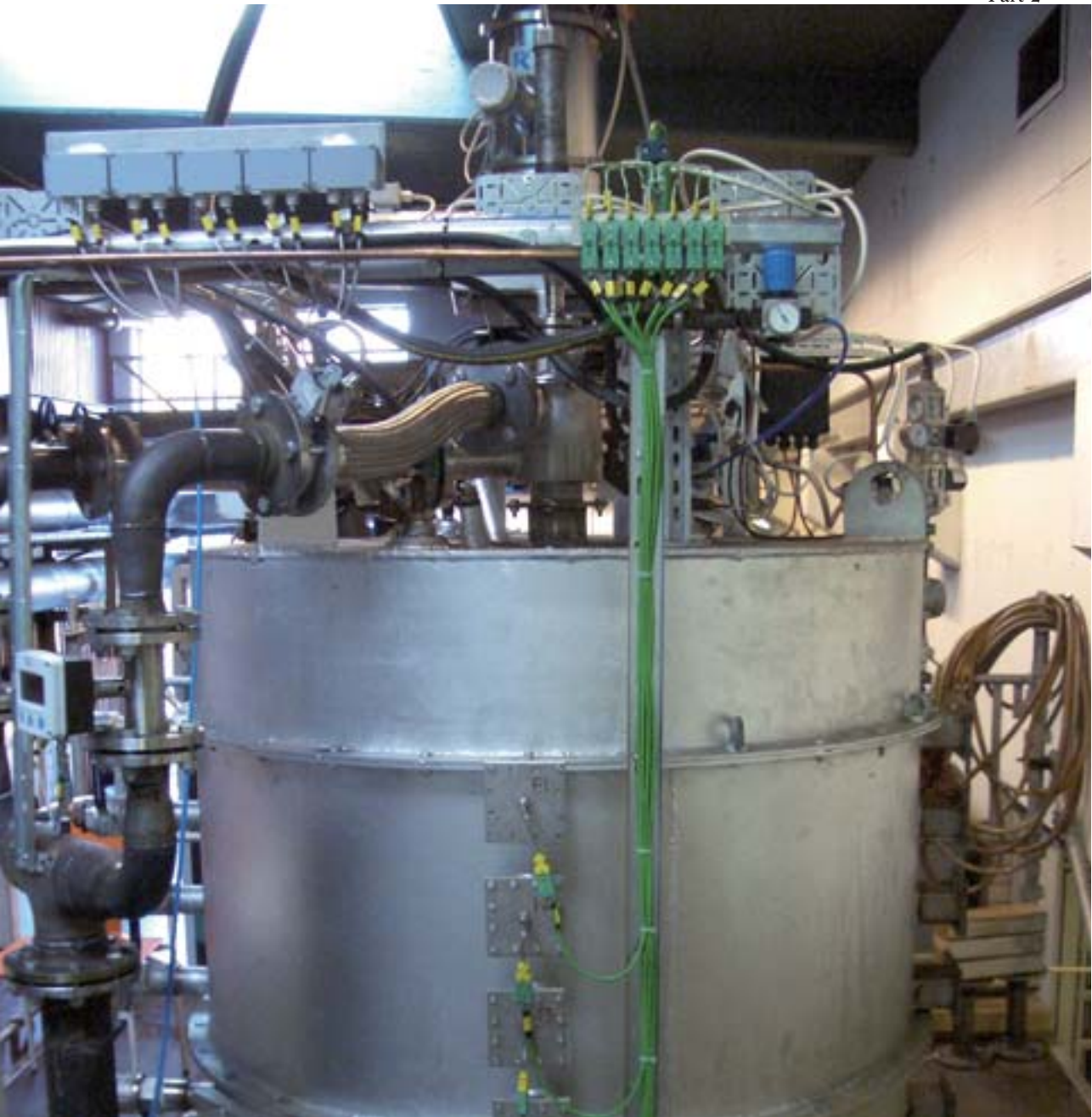
### **Difference in radiative properties**

Such data is required in order to assess the difference in radiative properties in terms of emissivity between air and oxy-fuel combustion, for different types of fuels with the overall aim of evaluating the accuracy of radiation models presently used in commercial CFD codes. Tests on both natural gas-fired and coal-fired conditions in air and oxy-fuel have been performed, which include measurements of the axial distribution of the hemispheric heat flux using an ellipsoidal radiometer. Since, for refractory lined furnaces, such as the one used in the work presented here as well as in the experimental studies carried out previously, the dominating contribution to the local incident radiative flux originates from the surrounding walls, which makes the analysis of hemispheric heat flux data less interesting. This due to that the inner

wall surface temperature between different test conditions is bound to change from air to oxy-fuel conditions, and, that the wall emissivity, for these types of materials and temperatures, will approach unity. The wall dominance on hemispheric radiation measurements is further accentuated for moderate and non-sooty flames with low emissivity of the flame envelope. In one of the previous studies this set back of the ellipsoidal radiometer measurements was recognized and it was concluded that, in order to determine the flame radiation characteristics of oxy-fuel combustion in a more accurate manner, wall effects should be minimized to facilitate a direct comparison between oxy-fuel and air-fired conditions.

### **Detailed profiles**

Hence, in this work the aim is to reduce the influence of the hot furnace walls on the radiation data. The study comprises uni-directional measurements of the radiation intensity in order to facilitate the possibility to interpret the difference between the three test environments. In addition, detailed profiles on temperatures and gas concentrations have been measured to characterize the properties of the different flames and to facilitate a more detailed discussion of the flame emissivity in relation to the radiation profiles.



The upper part of the Chalmers oxy-fuel combustor. To the left the pipes of the primary and secondary streams are seen, which feed the top mounted burner with either air or a mixture consisting of oxygen and carbon dioxide.

# Experimental facility and test conditions

Figure 2 shows the 100 kW oxy-fuel combustion test unit located in connection to the Chalmers 12 MW research boiler, thus taking advantage of the existing measurement infrastructure. The test unit has specifically been designed for the study of oxy-fuel combustion under real flue gas recycling conditions. In this work, gas-fired tests were carried out with a fuel input of about 80 kW. The test conditions and fuel properties are specified in Table 2 and Table 3, respectively. The cylindrical refractory lined reactor is down-fired with an inner diameter of 0.8 meters and total height of 3.0 meters. The tests can be run under oxy-fuel conditions (with different mixing ratios between oxygen and carbon dioxide/water), with air or with oxygen enriched combustion, with the latter condition by means of direct oxygen injection in the burner. The flue gas recycle loop includes one separate temperature controlled cooler and one condenser enabling both wet and dry flue gas recycling (Figure 2). In this work, dry flue gas recycling conditions was applied. The flue gas temperature after the condenser is reduced to about 25 to 30°C corresponding to 2 to 2.5 volumepercent

moisture content in the recycled flue gas, and thus similar to non-preheated air-fired conditions. The ratio of the volumetric flow between the recycle stream and the stack gas is set by two frequency controlled ID-fans.

For the experiments given in this paper, the oxygen is mixed into the recycled flue gas up-streams the ID-fan in the recycle loop. After passing through the recycle fan the feed gas is divided into a primary and a secondary stream which then enters the two respective registers of the burner. Approximately 40 percent of the total flow enters the primary register. The ratio between the primary and secondary stream is adjusted by individual valve settings and the volumetric flows are continuously logged by turbine flow meters. Both oxygen and propane is supplied from bundles of gas tubes. The oxygen and propane flows are controlled by electronic mass flow meters.

In order to reduce the time for the combustor to reach thermal steady state conditions, cooling tubes with variable length and an outer diameter of 50 mm are inserted from the top of the combustion chamber at four positions close to the wall, equally

distanced from the flame. The temperature and flow rate of the incoming and outgoing cooling water is continuously measured for heat balance and modeling purposes. Wall temperature conditions are monitored by means of thermocouples measuring the temperature 20 mm from the inner wall surface at 2x7 positions at each side of the probe ports R1 to R7 (Table 1). The ports along the side of the furnace are used for in-furnace data collection, by means of water-cooled probes. A number of ports are available down stream of the reactor exit and at various positions in the flue gas recycle pass, which allow for flue gas as well as recycle feed gas composition measurements.

**Table 1. Measurement positions on the Chalmers 100 kW oxy-fuel unit**

Port number	Distance from burner [mm]
R1	46
R2	215
R3	384
R4	553
R5	800
R6	998
R7	1400

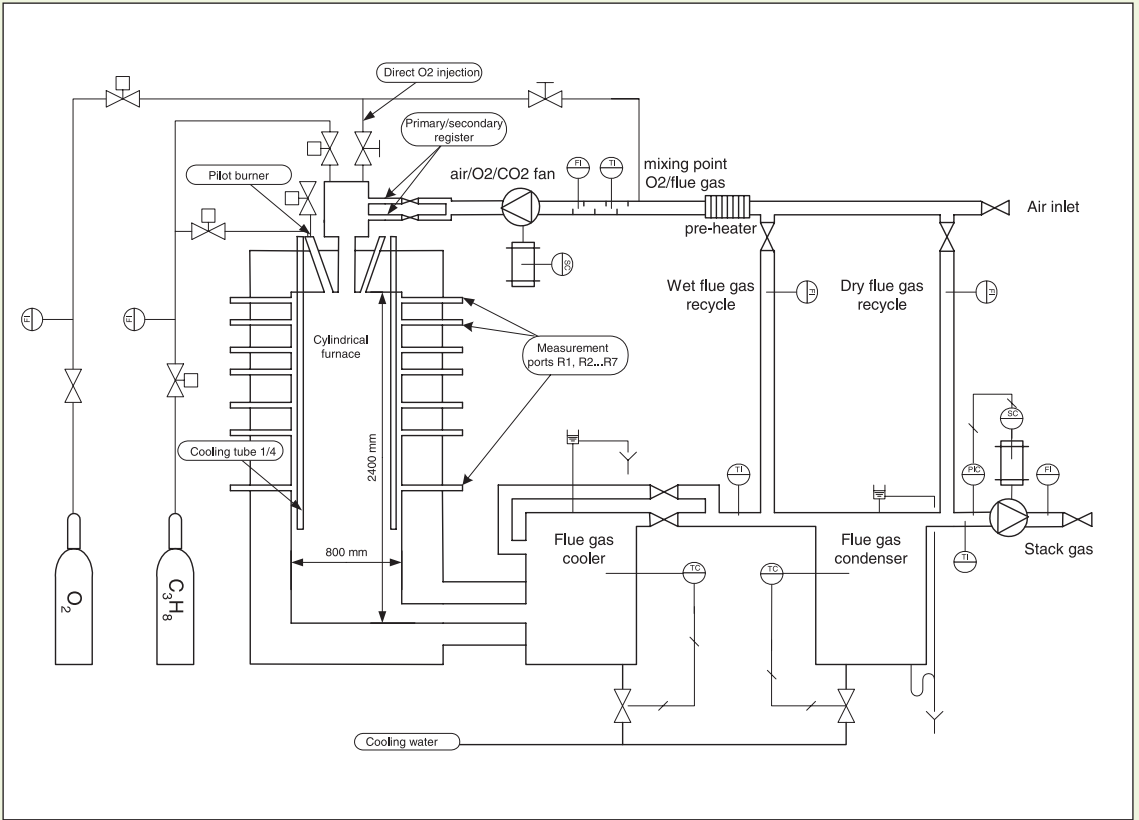


**Figure 2.** Schematic of the CHALMERS 100 kW oxy-fuel combustion test unit, which has been adopted for both gas and coal firing.

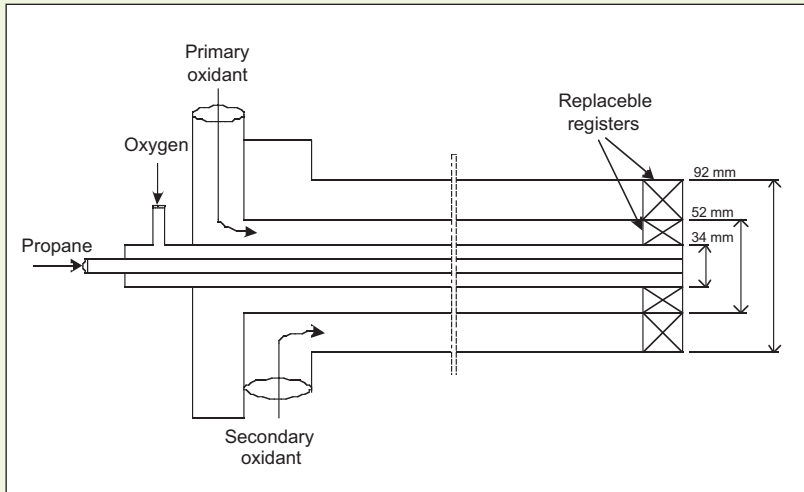


**Figure 3.** Schematic side view of the gas-fired burner.

The gas-fired burner (Figure 3) consists of two separate lances for fuel and direct oxygen injection (as mentioned, the oxygen register is not used in these tests). The primary and secondary swirl registers are replaceable in order to facilitate a change of the swirl number settings and the corresponding mixing conditions of the flame. Table 2 lists the settings used in the present work together with the overall test conditions of the measurements.

The tests comprise a reference test in air and two oxy-fuel test cases with different recycled feed gas mixture concentrations of oxygen (21 and 27 volume-percent) and carbon dioxide

(79 and 73 volume-percent). The 21 volume-percent oxygen case (OF 21 case) was chosen to keep the volumetric flow conditions similar to the air case whereas the 27 volume-percent oxygen case (OF 27 case) should give a temperature level similar to air-fired conditions. In-furnace gas concentration, temperature and total radiation (uni-directional) profiles are presented and discussed.

All tests were performed at a stoichiometric ratio of 1.15 resulting in a target oxygen excess of 3.0 volume-percent for the air and the OF 21 cases, and 3.8 volume-percent for the OF 27 case. The higher oxygen excess

in the latter case is due to that the volumetric flow of recycled flue gas is more than 20 percent lower than in the OF 21 case. For the OF 27 case the residence time is increased by the reduction in volumetric flue gas flow and to some extent also by the change in temperature distribution from air to oxy-fuel fired conditions. From the experimental results it is seen that the in-flame temperature distributions of the OF27 and the reference case are rather similar, that is the difference in temperature will only moderately influence the relative change in residence time from the air to the OF 27 case, whereas this change will be more pronounced under the OF 21 conditions. All in-furnace measurements have been repeated twice in order to ensure satisfactory repeatability for each test condition.

**Table 2. Test conditions for the gas-fired tests**

Heat input	80 kWth
Fuel	C <sub>3</sub> H <sub>8</sub>
Stoich ratio	1.15
Primary register	Fin angle 45 Swirl No 0.79
Secondary register	Fin angle 15 Swirl No 0,21

**Table 3. Test conditions for the three test cases**

Test case	Combustion media	Temp feed gas [°C]	Feed gas composition (vol %)			Theoretic CO <sub>2</sub> conc. @ stack (vol %)
			O <sub>2</sub>	N <sub>2</sub>	CO <sub>2</sub>	
Air	air	25-30	21	79	-	12
OF21	O <sub>2</sub> /CO <sub>2</sub> dry recycle	25-30	21	-	79	97
OF27	O <sub>2</sub> /CO <sub>2</sub> dry recycle	25-30	27	-	73	96

**Table 4. Fuel composition and oxygen quality**

Fuel analysis [average mole content]		
Methane	0	mol %
Ethane	< 0.1	mol %
Propane	98.3	mol %
Butanes	1.1	mol %
Pentanes & higher	< 0.1	mol %
Total Unsaturated HC	< 0.1	mol %
Sulphur	< 1	mg/kg
Hi	46.4	MJ/kg
Oxygen		
Quality (industrial std)	2.5	-
Oxygen content	99.5	vol%



# Measurements

## Gas concentration measurements

Measurements of in-furnace gas concentrations, temperatures and uni-directional radiation intensity were carried out to characterize the three test cases specified in Table 3. Gas composition data consisting of oxygen, carbon monoxide, carbon dioxide and total hydrocarbon concentrations are withdrawn from the furnace by means of a gas suction probe inserted in the probe ports and at the furnace exit. The hydrocarbon is measured as methane equivalents by means of an FID (flame ionization detector) based instrument. The analysis of oxygen,

carbon monoxide, and carbon dioxide were each performed for two different instruments with different measurement ranges, adapted for reference and oxy-fuel conditions respectively. The measurement principles of both oxygen instruments are of paramagnetic type, carbon monoxide is analyzed based on NDIR (non-dispersive infrared absorption) and carbon dioxide is measured based on NDIR and TC (thermal conductivity).

The gas suction probe is shown in Figure 4 and consists of a heated inner tube with controlled temperature to prevent condensation inside the probe

and an outer protecting water-cooled jacket with a diameter of 45 mm. The gas is dried and filtered before it is fed into the on-line gas analyzer train. The gas analysis instruments used are specified in Table 5. In order to avoid air-infiltration during the measurements, the furnace is maintained at an excess pressure of 20 to 50 Pa depending on the test condition. The oxygen excess in the stack gas is monitored throughout the suction measurements in order to control and maintain stable test conditions.

**Table 5. Gas analysis instruments**

Component	Manufacturer/ model	Measure- ment principle	Measure- ment range	Detection limit (of full range)	Span gas concentra- tion
O <sub>2</sub>	Fisher Rosemount (NGA 2000)	Para- magnetic	0–25 %	≤1%	9.00 %
	Binos (100 2M)	Para- magnetic	0–50 %	≤1%	21.0 %
CO <sub>2</sub>	Hartmann & Braun (Uras 10p)	NDIR	0–20 %	≤1%	18.0 %
	Binos (100 2M)	TC	0–100 %	≤2%	86.0 %
CO	Hartmann & Braun (Uras 10P)	NDIR	0–1.0 %	≤1%	8998 ppm
	Hartmann & Braun (Uras 3K)	NDIR	0–10 %	≤1 %	8.98 %
HC	Rosemount Analytical (400 A)	FID	0–10 %	≤2%	4.94%

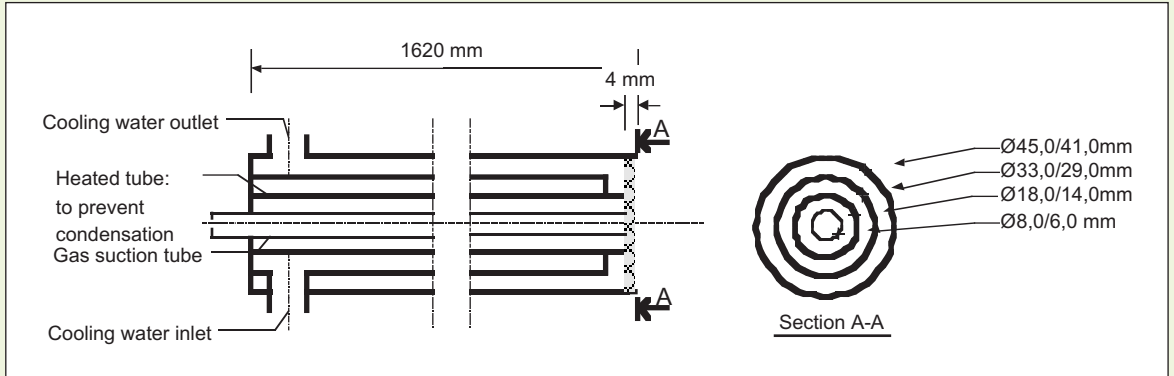


**Figure 4.** Schematic illustration of the gas sampling probe.

### Temperature measurements

The in-furnace temperature measurements were performed with a water-cooled suction pyrometer, shown in Figure 5. The probe is specifically designed for measurements of flame temperatures. The tip of the probe consists of a 200 mm long ceramic tube with an inner diameter of 10 mm in which a Pt-PtRh 30 percent-thermo-

couple (ANSI Type B) is placed, which measures temperatures up to 1700°C. The gas is sucked through a 6 mm hole on the side of the tube. To minimize the error due to radiation losses from the thermocouple the gas passes the thermocouple at high velocity. At 700°C, i.e. the lower furnace temperatures, the suction velocity is approximately 130 m/s. The velocity

increases up to about 230 m/s at 1500°C, that is the highest furnace temperatures represented in the flame zone of the present tests. Given that the probe is properly designed and that suction velocity is kept above 100 m/s, it is considered that suction pyrometry produces a maximum measurement error of about 50 K.

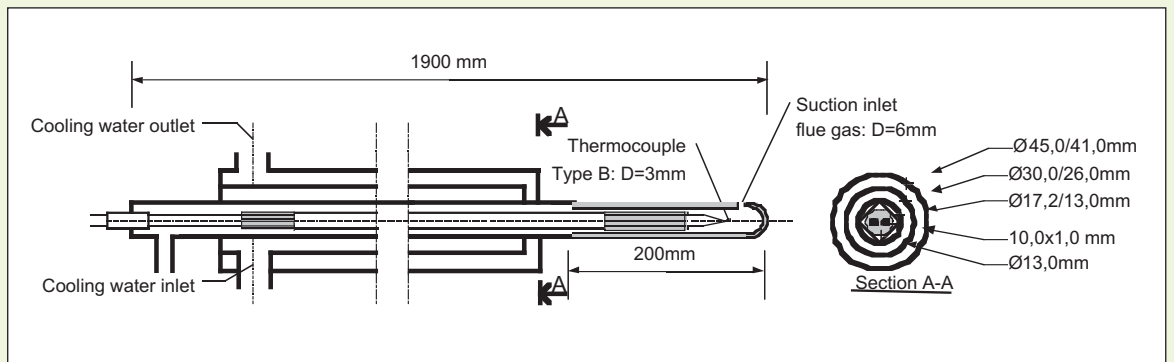


**Figure 5.** Schematic illustration of the suction pyrometer used for temperature measurements.

### Radiation intensity measurements

The radiation intensity measurements were carried out using a narrow angle radiometer of IFRF-type (Figure 6).

The probe consists of a straight tube, termed collimating tube, of 10 mm inner diameter, approximately 2 m long covered by a protecting water-cooled jacket. A temperature controlled receiver unit is located at the rear end of the collimating tube. The radiation beam passes through the collimating tube in which a number of parallel baffles are mounted to limit the bundle of rays and to restrict the view-

ing angle of the radiometer. In addition, the inner surface is blackened to minimize internal reflections. The beam reaches a high broadband reflectance mirror at the receiver end of the probe, which focuses the beam onto a thermopile. A shutter is placed between the receiver unit and the collimating tube to avoid an increase in the detector temperature and to enable zero check during traversing measurements of the flame. A known purge gas flow is applied during both calibration and measurements to prohibit radiating species and other contaminants to

enter the probe. The sensitivity of the signal to different purge gas flow rates was evaluated both during calibration and measurements in order to find the minimum applicable flow to restrict the influence from the purging on the in-situ measurement conditions. In the present probe setup Argon was used as purge gas at a flow rate of  $10\text{ l}_n^3/\text{min}$ . The calibration of the narrow angle probe was performed in a black-body furnace before and after each measurement series to check the zero drift of the thermal detector.

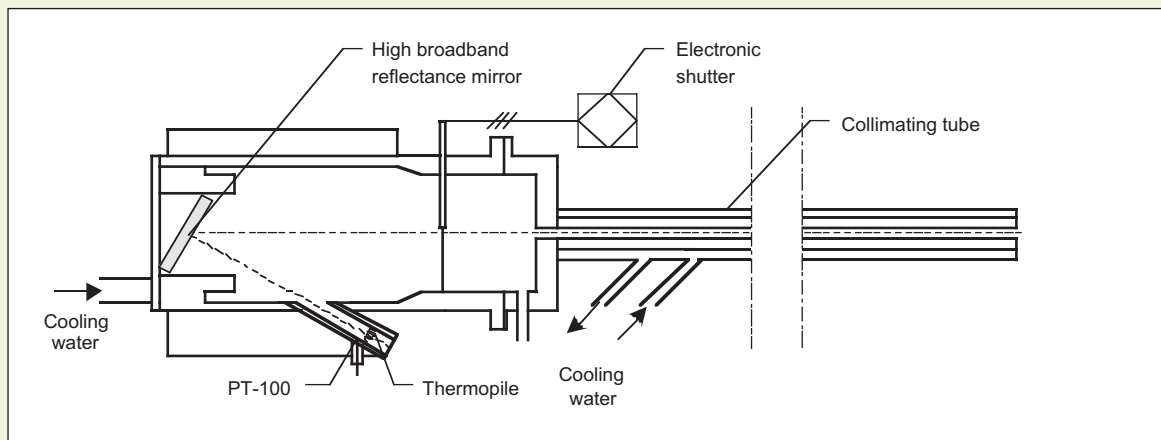


**Figure 6.** Schematic illustration of the narrow angle radiometer (IFRF type) used for total radiation measurements.

# Results and discussion

Figure 7 shows a typical start-up sequence from air-fired conditions to oxy-fuel combustion, in this case for the OF 21 case with a target oxygen excess of 3 volume-percent in the flue gas.

## Ninety percent carbon dioxide within thirty minutes

The oxygen and carbon dioxide concentrations are measured at the furnace exit. The step-wise changes in those locations are due to instrument adjustments (flow or pressure). It can be seen that a high level of carbon dioxide enrichment in the flue gas (85 to 90 vol %) is reached within the first 30 minutes.

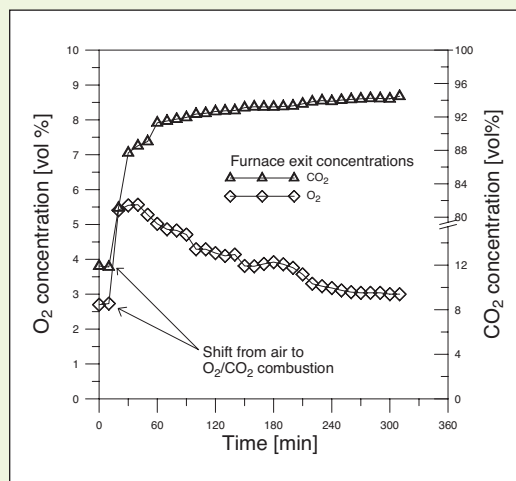
## Stable O<sub>2</sub> – more time consuming

The final depletion of the nitrogen content to reach stable oxygen excess concentration is rather time consuming. Satisfactory experimental conditions are typically reached after some four to five hours. Any discrepancy between the theoretic carbon dioxide concentration level (97 volume-percent) and the one measured (typically about 94 to 95 volume-percent) is therefore due to nitrogen still left in the recycling media, and, to some extent also due to the instrument precision of the carbon dioxide analyzer which has a maximum error of  $\pm 2$  percent of the full measurement range (0–100 percent).

It has been well established experimentally, that for a similar feed gas mixture in terms of volumetric concentrations oxy-fuel conditions yields significantly lower peak as well as overall combustion temperature levels than oxygen/nitrogen conditions (i.e. reference conditions). This is also the general impression obtained from a comparison of the OF 21 case and the air case.

## The highest measured combustion temperatures

For example, the highest measured combustion temperatures for the OF 21 and air-fired case in port R2 are approximately 1370°C and 1550°C, respectively. The lower temperature in the OF21 case is mainly a result from that carbon dioxide has higher specific heat capacity than nitrogen and to a certain extent, that there is an increase in radiation losses caused by the carbon dioxide which increases the gas emissivity. The significance of the latter effect obviously depends on the radiative properties of the flame considered, that is to what extent the contribution from moisture, soot and



## Temperature profiles

The centerline and radial temperature profiles are measured for the three different cases:

- air
- OF 21
- OF 27

**Figure 7.** Measured O<sub>2</sub> and CO<sub>2</sub> concentrations at the furnace exit during a start-up sequence from air to OF21-fired conditions.

particle content need to be included. The change in emissivity of the oxy-fuel environment is further discussed below, and related to the radiation intensity profiles.

### Improvement of the combustion intensity

A reduction of the recycled flue gas is an obvious way to increase reactor temperature levels in order to improve the combustion intensity, in this case from the OF 21 to the OF 27 case. As a result the combustion temperatures of the OF 27 case and the air case are rather similar, but different from the

OF 21 case which yields significantly lower temperatures of the combusting flow due to the cooling from the recycled carbon dioxide. Both the air and the OF 27 cases exhibit a strong negative gradient in temperature between 50 and 100 mm from the centerline, which represents the location of the flame front. In the OF 21 case the temperature starts to decrease already between the centerline and 50 mm distance away from the centerline (0 mm), and no parabolic shape of the temperature profile can be seen close to the centerline (the distributions are assumed axi-symmetric).

### A shift in position of the flame front

Although a weak trend of such a parabolic temperature distribution may exist between 0 and 50 mm, the tendency in ports R2 and R3 clearly shows a shift in position of the flame front. In addition, already between 50 and 100 mm the temperature is brought down to a level of about 700°C, which corresponds to the gas temperature near the wall (400 mm) of both the OF 27 and the air-fired case.

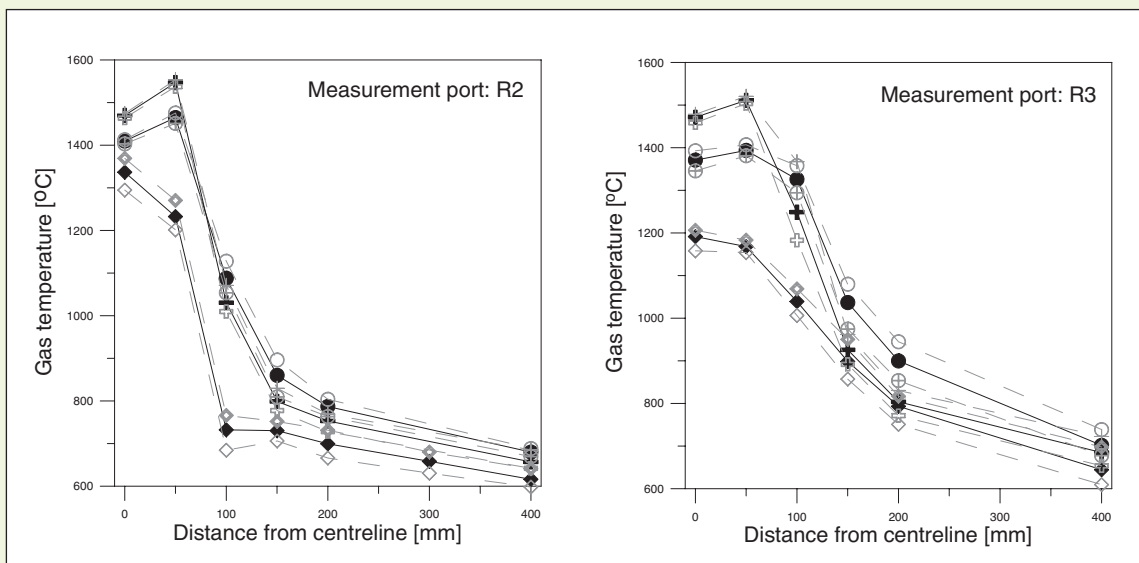
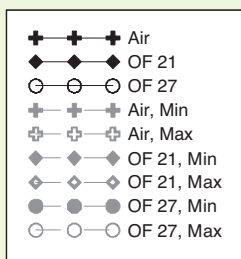


**Figure 8.** Measured mean, minimum and maximum radial temperature profiles in measurement ports R2-R3.



### Burn-out rate

This shows that for the OF 21 case, the physical volume of the high temperature zone is smaller for the OF 21 case compared to the two other cases and, as will be discussed later on, this influences the burn-out rate in the OF 21 environment. It should be noted that the measurement data representing the first position, R1, close to the burner, is accompanied with a high degree of uncertainty since the suction flow from the temperature probe is bound to disturb the flame, which is confirmed by a heavily fluctuating oxygen signal in the flue gas leaving the furnace when measurements are carried out in this position. Thus, the values from this position should be considered only as an indication of ignition not yet being initialized. Also,

the exact point of ignition cannot be detected, since for all cases the point is somewhere between the first and the second measurement port.

### The furnace wall temperatures

The furnace wall temperatures for the three cases, measured with thermocouples at a distance 20 mm from the inner furnace wall surface together with the minimum and maximum gas temperature, measured close to the inner furnace wall surface with the suction pyrometer. The furnace wall temperatures are measured at the right and left hand side of the probe ports on the same axial distances from the burner as shown in Table 1. The distribution of gas and wall temperatures correlate well for all three cases with the highest gas and wall temper-

atures obtained in the OF 27 case at a distance of 800 mm from the burner, where the temperature drops faster than for both air and OF 21.

### Gas concentration profiles

Radial gas concentration profiles consisting of oxygen, carbon monoxide and hydrocarbon. The difference in mass feed rate of air compared to the mixtures of oxygen and carbon dioxide results in different mass flux profiles. Still, the gas profiles and the burnout rates show clear trends and are consistent with the temperature profiles presented.

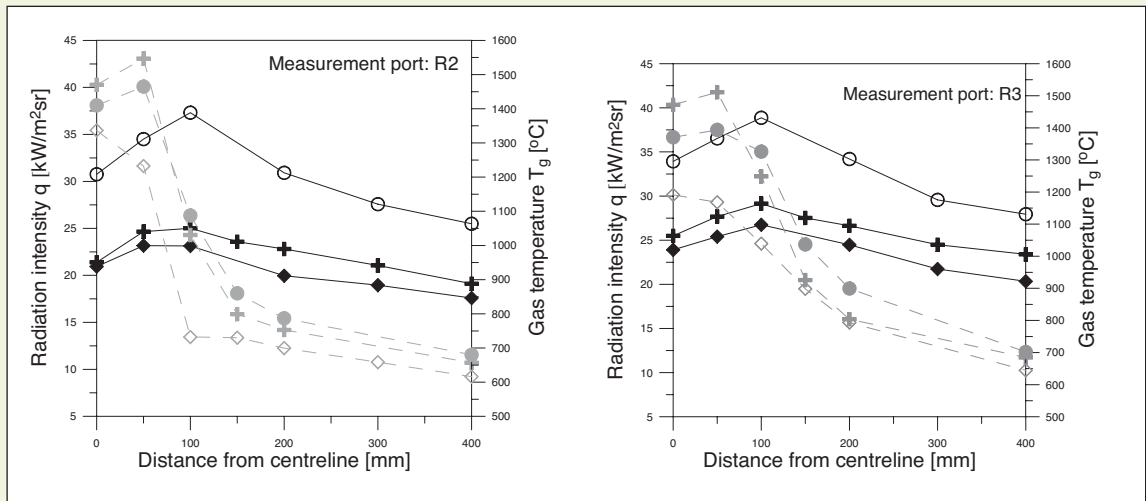
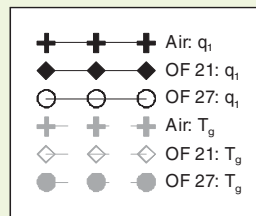


**Figure 9.** Mean values of the measured radial radiation intensity profiles with hot refractory furnace wall as background. The grey dotted profiles show the corresponding gas temperatures (also shown in Figure 8).



The results show that the gas composition of the flame envelope of the OF 21 case is clearly different from the two other cases. The amount of unburned hydrocarbons is significantly higher for the OF 21 case and, as a consequence, oxygen is still present in the flame core (i.e. oxygen from the recirculation motion of the flame). The suppressed development of the OF 21 flame is further seen in the carbon monoxide profiles that give significantly lower concentration levels compared to the air and OF 27 cases. The decline in combustion stability and performance of the OF 21 case can to a large extent be attributed to the reduced temperature levels compared to the other two cases, as shown in figure 8, and is caused by the high specific heat of carbon dioxide. It should be noted that the gas concentration and temperature data from intrusive measurement instruments such as the ones used here are rather collected from a measurement volume than an exact position. This applies to the gas suction probes and suction pyrometers employed here, especially the latter probe due to the rather high suction velocity as described above.

This is especially important to keep in mind for regions with sharp gradients, for example when comparing the hydrocarbon profiles and the temperature profiles in one of the figures above, where the high concentration of unburned fuel at 50 mm from the centerline can be explained by the fact that it corresponds to temperatures represented within a distance from 50 to 100 mm from the centerline, that is somewhere in the range between 700 to 1200°C, rather

than the exact same position as the temperature measurement at 50 mm. Compared to the OF 21 case the fuel burn-out of the OF 27 case is favoured by the increased temperature level and improved mixing conditions between fuel and oxygen, due to the reduced flue gas recycle. The hydrocarbon levels are low and the oxygen profile at the centerline exhibit a similar distinct zero-level as for air-fired conditions.

### Radiation intensity

The radial distributions (from the centerline to the probe wall) of unidirectional total radiation intensity have been measured for the three cases using the narrow angle radiometer. The maximum measured radiation intensity 100 mm from the centerline is recorded close to the flame boundary as indicated by the temperature profiles. Moving towards the probe wall to the right the intensity drops, as the absorption becomes higher than the emission.

### Difference in emissivity

The information from the temperature distributions shown previously together with the radial profiles of radiation suggests a change in emissivity for an oxy-fuel environment compared to reference conditions in air. As seen the radiation intensity is higher in the OF 27 case than in the air case despite the fact that the radial temperature levels are generally lower or similar to those of air and, in spite of the overall lower temperature levels, the radiation intensity profiles of the OF 21 case have a close resemblance to those of air. The obvious physical difference between the air case and oxy-fuel

conditions is the increase in carbon dioxide partial pressure (approximately 8 times the concentration level of normal air-fired conditions), from which an increase in gas band radiation is anticipated. The difference in total emissivity and in gas emissivity will therefore be compared between the oxy-fuel and the air case in order to OF 27 evaluate if the increase in overall emissivity can be attributed to an increase in oxygen band radiation only. The oxy-fuel environment is represented by the OF 27 case; since the experimental radiation data is restricted for the OF 21 case (i.e. no measurement data is available on q2 – see appendix).

It should be noted that differences in local emissivity may exist between OF 21 and OF 27 conditions since the soot formation may change from one oxy-fuel atmosphere to another. In fact, by comparing the shape of the radiation intensity profiles it is seen that the peak intensity 100 mm from the centerline is clearly accentuated for the OF 27 condition compared to the two other cases. This may indicate local differences in emissivity between the tests conditions, which could be caused by changes in soot volume fraction. Still, a local increase in temperature (between 50 and 100 mm) for the OF 27 case would cause the same effect and, hence, the spatial distribution of the measurements needs to be improved to further evaluate the local properties of the flames.

The equations and parameters are defined in appendix.

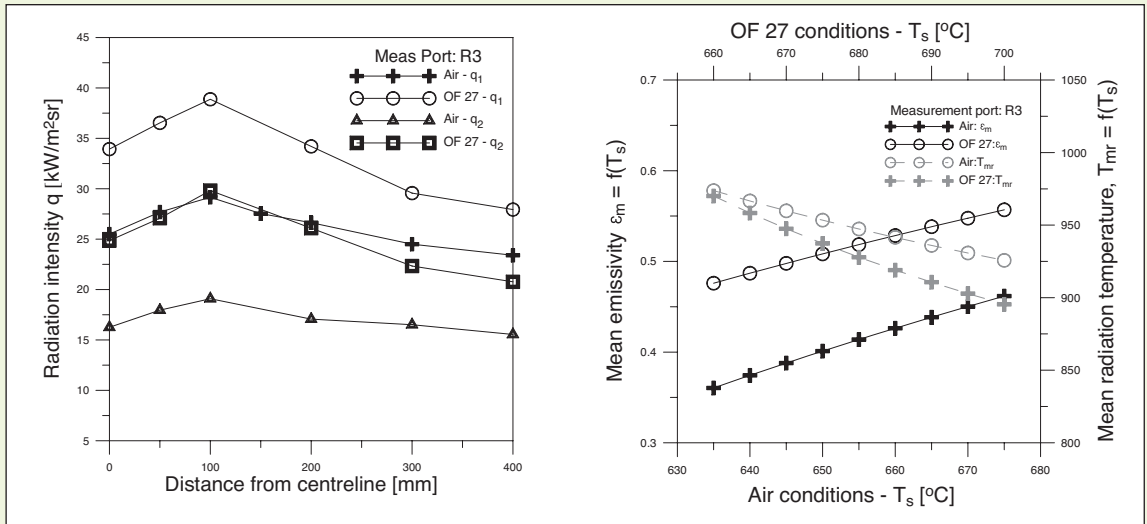


**Figure 10.** Radiation intensity, mean flame emissivity and average flame radiation temperature  
 a) Comparison of radiation intensity profiles, air and OF 27 conditions, measured against both cold black body target ( $q_2$ ) and hot refractory furnace wall ( $q_1$ ) in port R3.  
 b)  $T_{mr}$  and  $\epsilon_m$  based on the measurements given in Figure a and calculated as a function of different furnace wall temperatures (Air:  $655 \pm 20^\circ\text{C}$  and OF 27:  $680 \pm 20^\circ\text{C}$ ).

The left figure above shows a comparison of radiation intensity profiles for air and OF 27 conditions in port R3, measured against both a cold black body target, which represents the term  $q_2$  in Eq. (9), and the hot refractory lined furnace wall, that is  $q_1$  in Eq. (9). These data together with the radiation intensity reading of the background wall alone,  $q_3$  in Eq. (9), is used to determine the mean flame emissivity,  $\epsilon_m$ , and an average flame radiation temperature,  $T_{mr}$ , for the OF 27 and air-fired conditions, respectively. (The equations are presented in the appendix "Theory"). The results are presented in the right figure above, where  $\epsilon_m$  and  $T_{mr}$  are plotted as a

function of the background furnace wall temperature. For the calculation the radiation intensities at 400 mm from the centerline are used, since the furnace cross sectional emissivity is of interest. As seen, the accuracy of the surface wall temperature prediction is critical, but given that the wall surface temperature prediction is correct for both cases, that is  $655^\circ\text{C}$  for air case and  $680^\circ\text{C}$  for the OF 27 case, the total emissivity becomes 0.41 and the mean radiation temperature becomes about  $930^\circ\text{C}$ , for the air-fired case and for the OF 27 case the total emissivity becomes 0.52 and the mean radiation temperature becomes approximately  $950^\circ\text{C}$ .

### Wall intensity

There was a difficulty to obtain a stable radiation intensity signal from the furnace wall alone (i.e.  $q_3$ ) since the water-cooling of the probe cool down the wall as soon as the probe is positioned close to the wall. Therefore, the measurements of wall radiation intensity was repeated twice for the air-fired test condition in port R3 with a measured intensity of  $13.4 \pm 0.4$  kW/m<sup>2</sup>sr which together with  $\epsilon_b = 1$  corresponds to an inner wall surface temperature of  $655^\circ\text{C}$  with an error margin of about  $\pm 10^\circ\text{C}$ . This repetition was however not carried out for the OF 27 condition, but instead the same temperature difference has been



assumed as for air-fired conditions, based on temperature measurements, over the 20 mm of refractory lining. The temperature level corresponding to probe port R3, in principle constant in time, is approximately 25°C higher for OF 27 conditions compared to those of air from which the inner wall surface temperature  $T_s$  has been estimated to 680±10°C for the OF 27 condition. Including the thermocouple measurement error this results in a total error margin of about ±20°C for the assumed wall temperatures.

### Input parameters for the gas emissivity model

Eqs (12) to (18) (presented in the appendix “Theory”) are used to determine the gas emissivity with the input parameters listed in the table 6, where the partial pressures of the two respective gases are assumed constant within the measurement volume. Compared to measurement data this assumption does not introduce any significant error. As previously described, the gas concentration measurements were performed on dry basis, and so the water vapour concentration is obtained from stoichiometric calculations with conditions as specified in Table 2–3 and fuel properties according to Table 4. The background surface temperatures are the same as in the right figure above, although the error margin has been disregarded, since in this case it has a negligible influence on the results. The path length of the gases is the same as the inner diameter of the furnace.

**Table 6. Input parameters, partial pressure ( $p_g$ ), background surface radiation temperature ( $T_s$ ) and path length ( $L$ ) to the gas emissivity model.**

Test case	$p_{CO_2}$	$p_{H_2O}$	$T_s$ [K]	$L$ [m]
Air	0,10	0,14	928	0,80
OF 27	0,82	0,18	953	0,80

### Gas emissivity modelling

Gas emissivity modeling with Eqs (12) to (18) shows that the emissivity of the water vapour is significant in both environments although dry flue gas recycling is applied, with air and OF 27 conditions. In fact, at lower gas temperatures  $\epsilon_{H_2O}$  is still dominating over  $\epsilon_{CO_2}$  also in the OF 27 case although the temperature dependence of  $\epsilon_{H_2O}$  reduces its importance at higher radiation temperatures such as in the near flame region. The measured gas temperatures in port R3 (see figure 8) show a close resemblance for the two cases as does the calculation of the mean radiation temperature in the right figure 10 above.

### Increased gas emissivity

For a similar mean gas temperature as the air case the OF 27 total gas emissivity is increased with about 20 to 30 percent for the relevant gas temperature interval, where the difference is accentuated at higher temperatures due to the stronger temperature dependence of  $\epsilon_{H_2O}$  compared  $\epsilon_{CO_2}$  for the conditions specified in Table 4. For example, with the mean radiation temperatures given in the right figure above, i.e. in the range between 930 to 950°C,  $\epsilon_g$  becomes 0.23 in the air-fired case and 0.29 in the OF 27 case. When comparing the absolute values of the change in  $\epsilon_m$  and  $\epsilon_g$  it is suggested that

for similar gas temperatures, the difference between the two combustion environments in terms of increased radiation intensity of the OF 27 case can partly, but not solely, be explained by an increased gas emissivity. Errors introduced in the calculation of  $\epsilon_m$  mainly due to the wall temperature prediction, as shown in the right figure above, and the grey gas approximation, as will be discussed below, can however not be neglected when comparing  $\epsilon_m$  and  $\epsilon_g$ . Still, the conclusion that the total emissivity of the OF 27 flame increases more than that suggested by an increased emissivity due to  $CO_2$ , is consistent with the measured radiation intensities for the OF 27 environment compared to air, where the net incident wall intensity ( $q_2$  in the left figure 10 above) increases with more than 30% despite similar temperature profiles for air and OF 27 conditions (Figure 8).

Another possible reason for the increased radiation intensity in the OF 27 case is the possibility that local high temperatures at the flame front may not have been detected due to the restricted spatial resolution of the measurement positions. Yet another reason is that the rate of soot production may increase from air to the OF 27 atmosphere.

### Reduced sooting tendency

The figures below display the difference in flame luminosity between the air-fired and the OF 21 case. As seen, the observations of the OF 21 flame to the right with its blue emission suggest that the sooting tendency is clearly reduced (soot creates the yellow light emission in a flame) compared to reference conditions. In fact, the background probe opening is clearly visible (the annular

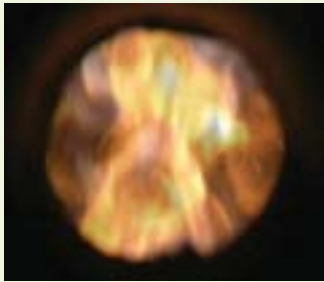
opening in the background) in the image of the OF 21 flame since the yellow light is only concentrated into thin sheets of the burning soot.

The background to these observations is supported by experimental findings reported in the literature suggesting a reduced soot production tendency when adding carbon dioxide on either fuel or

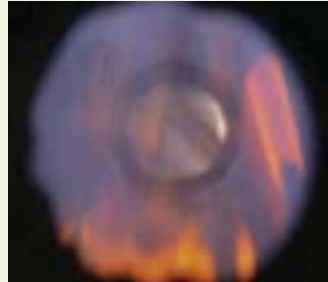
oxidizer side to a hydrocarbon diffusion flame. Soot production is dependent on the temperature and concentrations of soot-precursors and the soot reducing effects by carbon dioxide addition are reported to be due to both dilution and thermal as well as chemical effects. Hence, besides the direct effect with an increased gas band absorption by the carbon dioxide, the

CO<sub>2</sub> may also have significant effects on the soot formation during oxy-fuel conditions, hence causing secondary effects on the change in the radiative properties of the flame. Furthermore, visual observations in this work suggest that the black body radiation again increases from the OF 21 to the OF 27 case, but that the difference between air and OF 27 conditions are less clear.

a) Propane/air fired flame,  
3 percent oxygen excess



b) Propane/OF 21 fired flame,  
3 percent oxygen excess



Images showing the luminosity of propane fired flames in port No 2 (about 0.3 meters from the burner inlet). Figure 14a) shows the air-fired flames with an oxygen excess of 3 volume-percent in the flue gas and 14b) shows the OF 21 flame with an oxygen excess of 3 volume-percent.

### Further experimental work

The modeling shows that the maximum difference between the total gas emissivity and absorptivity for the reference condition in air is approximately 10 percent when the gas temperature varies between 700°C and 1300°C with two different background temperatures: the background temperatures equal to the furnace wall temperature or to that of a cold black body target. It should be noted that the temperature of the cold black body is

below the strict applicable minimum temperature of the model. That is less than 400K, which may affect the accuracy of the results. The difference increases for the OF27 case with a maximum difference of about 25 percent between emissivity and absorptivity for the corresponding gas and background temperatures. Still, the results obtained from Eqs (9) and (10) in the appendix are consistent with the measurement data. The mean emissivity as determined by Eqs (9)

and (10) therefore serve as a useful comparison of the two combustion environments, i.e. air and OF 27 conditions, in relation to the total gas emissivities determined according to Eqs (12) to (18). In conclusion, in order to facilitate the use of more precise methods to locally determine the change in emissivity, measurements of temperature and radiation intensities with a higher spatial resolution are required. Further experimental work is therefore planned with this aim.

# On-going work on oxy-coal combustion

The work on gas-fired combustion tests is currently being followed up by tests with lignite as fuel. The focus of the lignite fired tests is partly the same as for the gas fired tests, that is the radiation properties of the flame and combustion gases, which will change drastically from those during the gas-fired tests, due to the properties of lignite as a fuel. The emission characteristics will however also be studied in detail in terms of for example the nitrogen chemistry as well as the build up of acidic components (sulfur dioxide and sulfur trioxide) in the recycle loop.

## Two images of the lignite flame

The figures (right) shows two images of the lignite flame for two different test environments with a significant difference in the amount of oxygen available in the combustion zone. The figure to the left shows an image of an oxygen rich oxy-fuel flame, with 10 volume-percent oxygen excess in the flue gas. The figure to the right demonstrates an air-fired flame with 3 volume-percent oxygen excess in the

flue gas. The image quality of the air-fired flame is affected due to a coal dust laden quartz window, but there is a clear difference in the light emission from the two flames, where the oxygen rich flame to the left is almost entirely white and much brighter than the air-fired flame. This is typical for oxygen rich flames, both gas and coal fired, and the colour of the flame has a significant importance on the radiative properties of the flame.

The color itself is due to the amount of soot, which is formed and thereafter burns, in the flame envelope as well as the corresponding combustion intensity and peak temperatures in the flame zone. The images in the figure can for example be compared with the photos in the previous section showing the flame emission from gas-fired oxy-fuel and air-flames. The OF 21 flame is dominated by the blue background emission and the corresponding temperature levels are significantly lower in this flame compared to the air fired flame. The latter flame is as seen instead dominated by the yellow light from the soot.

**a) Lignite/oxy-fuel flame with 10 volume-percent oxygen excess**



**b) Lignite/air flame with 3 volume-percent oxygen excess**



Side view of the flame at the burner inlet a) combustion of lignite in oxy-fuel flame with a high oxygen excess of 10 volume-percent and b) combustion of lignite in air with an oxygen excess at 3 volume-percent.

### Two side view images of the air-fired flame

The images (right) show two side views of the air-fired flame, from port no 2, which is about 0.3 meters from the burner inlet. The image to the left shows the flame during measurement with the suction probe, which delivers the gas samples from the combustion chamber to the gas analysis system for analysis of oxygen, carbon monoxide, carbon dioxide, total hydrocarbons, nitrogen oxide, nitrogen dioxide and sulfur dioxide in the standard set-up. As seen in the image to the left the flame structure is obviously affected by the probe compared to flame in the other image, where the probe has not yet been inserted. This underlines the importance of trying to minimize the different measurement systems effect on the test conditions, for example in terms of improved designs of the

sampling probes used for gas analysis, temperature measurements, radiation intensity measurements and particle concentration measurements etc. A prerequisite for such improvements is that the experiments are continuously followed up with modeling activities. Such modeling activities are being performed on the Chalmers test unit in a number of parallel projects. This work is carried out at Chalmers, but also at the University of Stuttgart, Fluent Europe Ltd and Vattenfall Utveckling AB. These activities aim to improve the knowledge on combustion and fluid dynamics modeling of oxy-fuel combustion to reach today's modeling standard of a normal air-fired flame. This, since the modelling tools are necessary for both predicting and evaluating the performance of a future full scale oxy-fuel power plant.

**a) Lignite/air flame with the suction probe inserted**



**b) Lignite/air flame without the suction probe**



Side view of the flame at port no 2 (approximately 0.3 m from the burner inlet) during combustion of lignite in air with an oxygen excess at 3.0 volume-percent. a) shows the disturbance of the gas suction probe on the flow field compared to the unaffected flow pattern in b).

# Conclusions

## To improve the knowledge

The overall aim of the experimental work presented in this paper is to improve the knowledge on the oxy-fuel combustion technique with respect to the flame characteristics with an emphasis put on the radiative heat transfer and burnout behavior. Recently performed tests with propane as fuel are presented, which comprise three different test cases: reference tests in air and two oxy-fuel test cases with different recycled feed gas concentrations of oxygen (21 and 27 volume-percent) and carbon dioxide (79 and 73 volume-percent). A reduction of the recycled flue gas media is a trivial way to increase reactor temperature levels in order to improve the combustion intensity, in this case from the OF 21 to the OF 27 case.

## The temperature levels

The temperature levels of the OF 21 flame are significantly lower than in the reference conditions in air due to the cooling by the recycled carbon dioxide, which results in a suppressed development of the OF 21 flame, which is seen from the profiles of oxygen, carbon monoxide and total hydrocarbon. Compared to the OF 21 case the fuel burn-out of the OF 27

case is favored by the increased temperature level and improved mixing conditions between fuel and oxygen and in general, the OF 27 case exhibits similar overall combustion behavior as the air-fired reference case in terms of gas concentration and temperature profiles. The systematic picture of the temperature and radiation profiles suggests a significant change in emissivity for the oxy-fuel environment compared to reference conditions in air. For example, the radiation intensity increases for the OF 27 case compared to air conditions despite the fact that the radial temperature levels are generally lower or similar to those of air. The difference in total mean emissivity compared to the difference in gas emissivity at similar mean radiation temperatures for the air and the OF 27 case suggest that the higher radiation intensity in the OF 27 case can partly, but not solely be explained by an increased gas emissivity.

## More detailed information is required

Moreover, in order to improve the interpretation of the changes between the different combustion environments, more detailed information on the spatial resolution of temperature and

radiation intensities are required in order to locally determine the change in emissivity. Further experimental work is planned with this aim for both gas and coal fired tests. The on-going experiments oxy-coal combustion is briefly summarized in this report. In these tests, the aim is to characterize the performance of Lausitz lignite (German brown coal) during oxy-fuel fired conditions compared to reference tests in air. A strong focus will be put on the radiation properties of the flame and combustion gases, just as for the previously performed tests with gas. The emission characteristics will however also be studied in detail, for example in terms of the nitrogen and sulphur chemistry. The experiments carried out at the Chalmers oxy-fuel test unit are carried out in parallel with modeling work in order to improve the overall understanding of the combustion process, and to develop design tools required in the process of building a 30-50 MWth pilot plant, and in the end, the demonstration of a full scale 600-1000 MWe oxy-fuel power plant with CO<sub>2</sub> capture.

# APPENDIX

## Theory

The following describes the interpretation of the radiation data obtained with the previously described narrow angle radiometer probe (in part 2) and the method to characterize the flame in terms of flame emissivity together with the gas emissivity model applied.

For the interpretation, measurements with the narrow angle probe were carried out both with the hot refractory lined furnace wall and a cold non-reflecting plate as backgrounds. The radiation intensity at any given distance  $d$  from the hot furnace wall to the probe end represents the sum of:

- i radiation from the flame and combustion gases received along the viewing path of the probe,
- ii background radiation from the hot refractory furnace wall, partly absorbed by the gas layer along the viewing path  $d$  of the probe, and
- iii in the background reflected radiation from the flame and combustion gases (i) partly absorbed within the interval  $d$ .

Thus, the total radiation intensity that reaches the probe can be expressed as:

$$q_1 = \int_0^{\infty} \varepsilon_{\lambda} R_{\lambda T_g} d\lambda + \varepsilon_b \int_0^{\infty} (1 - \varepsilon_{\lambda}) R_{\lambda T_s} d\lambda + (1 - \varepsilon_b) \int_0^{\infty} \varepsilon_{\lambda} (1 - \varepsilon_{\lambda}) R_{\lambda T_g} d\lambda \quad (1)$$

where  $q_1$  is the sum of contributions (i) to (iii) and the emissivity of the flame and combustion gases at a certain wavelength  $\lambda$  is treated as a general function of wavelength  $\lambda$  whereas the background wall emissivity  $\varepsilon_b$  is assumed constant. The function  $R_{\lambda T}$  gives, for a temperature  $T$  [K] and a wavelength interval  $\lambda$  to  $\lambda + d\lambda$ , the black body radiation  $R_{\lambda T} d\lambda$ . The temperatures,  $T_g$  and  $T_s$  are the gas and background wall temperatures, respectively.

At the measurement levels employed, the furnace wall temperature typically varies  $\pm 50^{\circ}\text{C}$  (around an average of  $600^{\circ}\text{C}$ ) in all three cases (as will be discussed below, the inner surface temperature increases slightly compared to the wall temperature measurements). This results in an emissivity of about 0.9 of the refractory lining material. However, with the low conductivity and considerable thickness of the furnace walls the conduction losses through the lining are negligible at thermal steady state conditions. Furthermore, on the wall surface, the convective term is small compared with the dominating radiative term. Thus, since the heat exchange is in principle only due to radiation the energy balance in Eqs (2) to (6) gives that the effective emissivity  $\varepsilon_b$  is equal to unity. With  $T_s$  being the temperature and  $Q$  the total incident heat flux of the wall surface in the energy balance the total outgoing heat flux  $Q^+$  can be written:

$$Q^+ = \varepsilon_b \sigma T_s^4 + (1 - \varepsilon_b) Q^- \quad (2)$$

According to the assumption above, all heat is exchanged by means of radiation and hence the rate of emission must equal the rate of absorption, from which follows,

$$\varepsilon_b \sigma T_s^4 = \varepsilon_b Q^- \quad (3)$$

$$Q^- = \sigma T_s^4 \quad (4)$$

$$Q^+ = \varepsilon_b \sigma T_s^4 + (1 - \varepsilon_b) Q^+ \quad (5)$$

$$Q^+ = \sigma T_s^4 \quad (6)$$

Thus, it is clear that the effective emissivity  $\varepsilon_b$  is 1 regardless of the actual emissivity of the material of the wall surface. Therefore, the reflected radiation (iii) can be left out without any significant error, and Eq. (1) can instead be written as:

$$q_1 = \int_0^{\infty} \varepsilon_\lambda R_{\lambda T_g} d\lambda + \int_0^{\infty} (1 - \varepsilon_\lambda) R_{\lambda T_s} d\lambda \quad (7)$$

Eqs (1) and (7) take into consideration the wavelength dependence of the emissivity of the flame/gas layer over which the total radiation measurement is carried out. However, the measured data do not give information on the spectral resolution of the radiation. Therefore a simplified treatment of the data is required in order to evaluate the difference in total emissivity between the air and the  $O_2/CO_2$ -environment, the latter being represented by the OF 27 case, due to restricted measurement data for the OF 21 case. Hence, for the air and the OF 27 case the total mean emissivity of the gas layer is determined, based on three separate measurements of the radiation intensity. The general basis of the method used to determine the mean emissivity is that the flame or gas layer is considered grey, so that the emissivity becomes independent of wavelength and equal to the absorptivity, independent of the relation between the gas and the background temperature. The scattering is neglected due to the small size of the soot particles and hence the emissivity is assumed equal to the absorption. These assumptions result in a flame emissivity independent of wavelength and, integrated over the spectrum, Eq. (7) can be written:

$$q_1 = \sigma \varepsilon_m T_{mr}^4 + \sigma (1 - \varepsilon_m) T_s^4 \quad (8)$$

where  $\varepsilon_m$  represents the mean emissivity and  $T_{mr}$  the average radiation temperature of the gas layer concerned, i.e. along the viewing path of the probe. In order to determine  $\varepsilon_m$  and  $T_{mr}$ , separate measurements of the radiation from the gas layer  $\sigma \varepsilon_m T_{mr}^4$  and the background furnace wall  $\sigma T_s^4$  in Eq. (8), are required in addition to measurements of  $q_1$ , a procedure which is followed in the present work. Hence, the term  $q_2$  is represented by the first term in Eq. (8). Together with the net contribution of the background wall,  $q_3$ , the mean emissivity and the mean radiation temperature of the gas layer can be calculated according to

$$\varepsilon_m = 1 - \frac{q_1 - q_2}{q_3} \quad (9)$$

$$T_{mr} = 4 \sqrt[4]{\frac{\pi q_2}{\varepsilon_m \sigma}} \quad (10)$$

Obviously, with  $T_{mr}$  and  $\varepsilon_m$  from Eqs (9) and (10) drastic simplifications are introduced compared to real conditions for which there is a spectrally dependant emissivity  $\varepsilon_\lambda$ , and non-uniform concentration and temperature profiles within the measurement volume. For example, the average radiation temperature of the furnace ( $T_{mr}$ ) should not be confused with the real average gas temperature. The grey approximation is also more questionable in the case of a gas-fired flame compared to a highly luminous oil flame. This since the gas band radiation will have a stronger impact on the total emissivity in a moderately sooting flame and cannot be neglected in comparison to the continuous radiation due to soot and especially so for oxy-fuel conditions. This implication on the results will be further discussed below.

#### Determination of total gas emissivity

As discussed above  $\varepsilon_m$  will include emission from both gas and soot. Therefore  $\varepsilon_m$  can be expressed as:

$$\varepsilon_m = \varepsilon_g + \varepsilon_s - M \varepsilon_g \varepsilon_s \quad (11)$$

where  $\varepsilon_g$  and  $\varepsilon_s$  are the gas and soot emissivities across the gas layer and the product  $\varepsilon_{gs}$  represents the band overlap of soot and gas. A reduction factor  $M$  should be introduced, which depends mainly on the gas temperature and to less extent on the soot volume fraction. This, since the emission bands of  $\text{CO}_2$  and  $\text{H}_2\text{O}$  are not randomly located in the spectrum and since the monochromatic soot emissivity increases with decreasing wavelength. A possible change in band overlap between soot and gas will however not be treated in this work, due to its small effect on the overall emissivity. There are no experimental data available on the soot volume fraction from the flames investigated in this work. Instead, in order to see if the difference in mean emissivity between the two combustion environments corresponds to the difference in gas emissivity, including  $\text{H}_2\text{O}$  and  $\text{CO}_2$  as radiating gases, the gas emissivity is determined using an existing model. This model was chosen since it accommodates a high degree of generality for which it has been recognised. This, since the  $\text{CO}_2$  and  $\text{H}_2\text{O}$  emissivities are treated separately and the total emissivity of the mixture is determined by taking a total band overlap correction term into consideration. Hence, any arbitrary partial pressures of  $\text{CO}_2$  and  $\text{H}_2\text{O}$  can be applied in the model. The polynomial correlations of the model produce a maximum error of 5 percent for water vapour and 10 percent for  $\text{CO}_2$  emissivities at a temperature above 400 K, compared to the spectral integration data upon which the model is based. The total emissivity for a mixture of  $\text{CO}_2$  and  $\text{H}_2\text{O}$  is obtained from:

$$\varepsilon_g = \varepsilon_{\text{CO}_2} + \varepsilon_{\text{H}_2\text{O}} - \Delta\varepsilon_{(\text{CO}_2 + \text{H}_2\text{O})} \quad (12)$$



In the model a zero partial pressure emissivity is given by the correlation:

$$\varepsilon_0(p_a L, p = 1bar, T_g) = \exp \left[ \sum_{i=0}^M \sum_{j=0}^N c_{ji} \left( \frac{T_g}{T_0} \right)^j \left( \log_{10} \frac{p_a L}{(p_a L)_0} \right)^i \right] \quad (13)$$

where  $T_g$  is the gas temperature,  $T_0 = 1000K$ ,  $p$  is the total pressure,  $p_a$  is the partial pressure and  $L$  is the path length of the gas, either  $CO_2$  or  $H_2O$ ,  $(p_a L)_0 = 1 \text{ bar cm}$  and  $C_{ji}$  are correlation constants. The emissivity for higher partial pressures, i.e. if  $p_a > 0$ , can then be calculated according to:

$$\frac{\varepsilon(p_a L, p, T_g)}{\varepsilon_0(p_a L, p = 1bar, T_g)} = 1 - \frac{(a-1)(1-P_E)}{a+b-1+P_E} \exp \left( -c \left[ \log_{10} \frac{(p_a L)_m}{p_a L} \right]^2 \right) \quad (14)$$

where  $a$ ,  $b$ ,  $c$  and  $(p_a L)_m$  are correlation parameters and PE is an equivalent pressure. For calculation of the total gas emissivity the last term in Eq. (12) needs to be considered, which is due to the band overlap of the two gases. This correction term is written

$$\Delta \varepsilon_{(CO_2+H_2O)} = \left[ \frac{\zeta}{10,7+101\zeta} - 0,0089\zeta^{10,4} \right] \left( \log_{10} \frac{(p_{CO_2} + p_{H_2O})L}{(p_a L)_0} \right)^{2,76} \quad (15)$$

with a partial pressure ratio  $\zeta$  defined as

$$\zeta = \frac{P_{H_2O}}{P_{H_2O} + P_{CO_2}} \quad (16)$$

The absorptivity is determined by multiplying a factor  $(T_g/T_s)^{0,5}$  to the emissivity evaluated at the external surface temperature  $T_s$  and a temperature scaled pressure path length according to:

$$\alpha(p_a L, p, T_g, T_s) = \left( \frac{T_g}{T_s} \right)^{0,5} \varepsilon \left( p_a L \frac{T_s}{T_g}, p, T_s \right) \quad (17)$$

and, finally, the total absorptivity of the gas mixture can be written:

$$\alpha_g = \alpha_{CO_2} + \alpha_{H_2O} - \Delta \varepsilon \left( p_{H_2O} L \frac{T_s}{T_g}, p_{CO_2} L \frac{T_s}{T_g} \right) \quad (18)$$

## Nomenclature

$a, b, c$	Correlation parameters	<i>Greek letters</i>	
$c_{ji}$	Correlation constants	$\alpha$	Absorptivity
$H_i$	Heating value, inferior [MJ/kg]	$\alpha_{\text{CO}_2}$	CO <sub>2</sub> absorptivity
$L$	Path length [cm]	$\alpha_{\text{H}_2\text{O}}$	H <sub>2</sub> O absorptivity
$M$	Reduction factor	$\alpha_g$	Gas absorptivity
$p$	Pressure [bar]	$\varepsilon_b$	Furnace wall emissivity
$p_a$	Partial pressure [bar]	$\varepsilon_m$	Mean emissivity
$P_E$	Equivalent pressure [bar]	$\varepsilon_g$	Total gas emissivity
$(p_a L)_m$	Correlation parameter	$\varepsilon_s$	Soot emissivity
$p_{\text{CO}_2}$	CO <sub>2</sub> partial pressure [bar]	$\varepsilon_\lambda$	Spectral emissivity
$p_{\text{H}_2\text{O}}$	H <sub>2</sub> O partial pressure [bar]	$\varepsilon_0$	Zero partial pressure emissivity
$q$	Radiation intensity [W/m <sup>2</sup> ,sr]	–	Partial pressure ratio: $p_{\text{H}_2\text{O}}/(p_{\text{CO}_2}+p_{\text{H}_2\text{O}})$
$q_1$	Radiation intensity from combustion gases and furnace wall [W/m <sup>2</sup> sr]	$s$	Boltzmann constant [W/m <sup>2</sup> K <sup>4</sup> ]
$q_2$	Radiation intensity from combustion gases [W/m <sup>2</sup> sr]	$l$	Stoichiometric ratio
$q_3$	Radiation intensity from furnace wall [W/m <sup>2</sup> sr]		
$Q^*$	Emitted heat flux [W/m <sup>2</sup> ]		
$Q^-$	Incident heat flux [W/m <sup>2</sup> ]		
$R_{\lambda,T}$	Gives, for a temperature $T$ [K] and a wavelength interval $\lambda$ to $\lambda + d\lambda$ , the black body radiation $R_{\lambda,T} d\lambda$		
$T_{BL}$	Measured furnace wall temperature LHS of the probe ports [°C]		
$T_{BR}$	Measured furnace wall temperature RHS of the probe ports [°C]		
$T_g$	Gas temperature [°C]		
$T_{gmin}$	Minimum gas temperature [°C]		
$T_{gmax}$	Maximum gas temperature [°C]		
$T_{mr}$	Mean radiation temperature [°C]		
$T_s$	Furnace wall temperature [°C]		

# Pathways to sustainable European energy systems

The European pathways project is a five year project with the overall aim to evaluate and propose robust pathways towards a sustainable energy system with respect to environmental, technical, economic and social issues. The focus is on the stationary energy system (power and heat) in the European setting. Evaluations will be based on a detailed description of the present energy system and follow how this can be developed into the future under a range of environmental, economic and infrastructure constraints. The proposed project is a response to the need for a large and long-term research project on European energy pathways, which can produce independent results to support decision makers in industry and in governmental organizations. Stakeholders for this project are: the European utility industry and other energy related industries, the European Commission, EU-Member State governments and their energy related boards and oil and gas companies. The overall question to be answered by the project is:

*How can pathways to a sustainable energy system be characterized and visualized and what are the consequences of these pathways with respect to the characteristics of the energy system as such (types of technologies, technical and economic barriers) and for society in general (security of supply, competitiveness and required policies)?*

This question is addressed on three levels; by means of energy systems analysis (technology assessment and technical-economic analysis), a multi-disciplinary analysis and an extended multi-disciplinary policy analysis. From a dialogue with stakeholders, the above question has been divided into sub-questions such as:

- What is the critical timing for decisions to ensure that a pathway to a sustainable energy system can be followed?
- What are "key" technologies and systems for the identified "pathways" - including identification of uncertainties and risks for technology lock-in effects?

- What requirements and consequences are imposed on the energy system in case of a high penetration of renewables?
- What are the consequences of a strong increase in the use of natural gas?
- What if efforts to develop CO<sub>2</sub> capture and storage fail?
- Where should the biomass be used – in the transportation sector or in the stationary energy system?
- Are the deregulated energy markets suitable to facilitate a development towards a sustainable energy system?
- Will energy efficiency be achieved through free market forces or regulatory action?
- What are the requirements of financing the energy infrastructure for the different pathways identified?

In order to address the sub-questions in an efficient and focussed way the project is structured into 10 work packages addressing topics such as description of the energy infrastructure, energy systems modelling, technology assessment of best available and future technologies and international fuel markets. In planning of the project significant efforts have been put into ensuring that the project should not only be strong in research but also in management, communication and fundraising.

The global dimension will be ensured through integration with the other three regional AGS pathway projects in the Americas, East Asia, and India and Africa.

More information at Pathways website:  
[www.ags.chalmers.se/pathways](http://www.ags.chalmers.se/pathways)



# The Alliance for Global Sustainability

The Alliance for Global Sustainability (AGS) brings together four of the world's leading technical universities – the Massachusetts Institute of Technology, The University of Tokyo, Chalmers University of Technology and the Swiss Federal Institute of Technology – to conduct research in collaboration with government and industry on some of society's greatest challenges.

The AGS represent a new synthesis of multidisciplinary and multi-geographical research that draws on the diverse

and complementary skills of the AGS partners. In addition to academic collaborations each of the universities has extensive experience in working with stakeholders, particularly a growing number of visionary leaders from industry who recognise their fundamental role in achieving sustainable development.

More information at AGS website:  
[globalsustainability.org](http://globalsustainability.org)



T O M

sista sida inlaga

slut